Projected Future Changes in Tropical Cyclones using the CMIP6 HighResMIP Multi-model Ensemble

Malcolm J Roberts[1], Alessio Bellucci[2], Benoit Vannière[3], Joanne Camp[4], Christopher David Roberts[5], Dian Putrashan[6], Jennifer Veronika Mecking[7], Kevin Hodges[3], Laurent Terray[8], Louis-Philippe Caron[9], Pier Luigi Vidale[10], Rein Haarsma[11], Retish Senan[12], Jon Seddon[4], Marie-Pierre Moine[13], Chihiro Kodama[14], Yohei Yamada[14], Colin M. Zarzycki[15], Paul Ullrich[16], Ryo Mizuta[17], Dan Fu[18], Gokhan Danabasoglu[19], Lixin Wu[20], Nan A. Rosenbloom[21], Qiuying Zhang[18], Enrico Scoccimarro[22], Fabrice Chauvin[23], Sophie Valcke[8], and Hong Wang[20]

[1]Met Office
[2]Centro Euro-Mediterraneo sui Cambiamenti Climatici
[3]University of Reading
[4]Met Office Hadley Centre
[5]ECMWF
[6]Max Planck Institute for Meteorology
[7]National Oceanography Centre Southampton
[8]CERFACS
[9]Barcelona Supercomputing Center
[10]NCAS Climate
[11]KNMI
[12]European Centre for Medium Range Weather Forecasts (ECMWF)
[13]CERFACS (Centre Européen de Recherche et de Formation Avancée en Calcul Scientifique)
[14]Japan Agency for Marine-Earth Science and Technology
[15]Pennsylvania State University
[16]University of California Davis
[17]Meteorological Research Institute
[18]Texas A&M University
[19]National Center for Atmospheric Research (NCAR)
[20]Ocean University of China
[21]National Center for Atmospheric Research (UCAR)
[22]Fondazione Centro euro-Mediterraneo sui Cambiamenti Climatici - CMCC
[23]Meteo France

November 21, 2022

Abstract

Future changes in tropical cyclone properties are an important component of climate change impacts and risk for many tropical and mid-latitude countries. In this study we assess the performance of a multi-model ensemble of climate models, at resolutions

ranging from 250km to 25km. We use a common experimental design including both atmosphere-only and coupled simulations run over the period 1950-2050, with two tracking algorithms applied uniformly across the models.

There are overall improvements in tropical cyclone frequency, spatial distribution and intensity in models at 25 km resolution, with several of them able to represent very intense storms. Projected tropical cyclone activity by 2050 generally declines in the South Indian Ocean, while changes in other ocean basins are more uncertain and sensitive to both tracking algorithm and imposed forcings. Coupled models with smaller biases suggest a slight increase in average TC 10m wind speeds by 2050.

Projected Future Changes in Tropical Cyclones using the CMIP6 HighResMIP Multi-model Ensemble

Malcolm John Roberts[1], Joanne Camp[1], Jon Seddon[1], Pier Luigi Vidale[2], Kevin Hodges[2], Benoit Vanniere[2], Jenny Mecking[3], Rein Haarsma[4], Alessio Bellucci[5], Enrico Scoccimarro[5], Louis-Philippe Caron[6], Fabrice Chauvin[7], Laurent Terray[8], Sophie Valcke[8], Marie-Pierre Moine[8], Dian Putrasahan[9], Christopher D. Roberts[10], Retish Senan[10], Colin Zarzycki[11], Paul Ullrich[12] , Yohei Yamada[13], Ryo Mizuta[14], Chihiro Kodama[13], Dan Fu[15,16] Qiuying Zhang[15,16], Gokhan Danabasoglu[17,16], Nan Rosenbloom[17,16], Hong Wang[18,16], Lixin Wu[18,16]

[1] Met Office, Exeter EX1 3PB, U.K. [2] National Centre for Atmospheric Science (NCAS), University of Reading, Reading, U.K. [3] University of Southampton, Southampton, U.K. (now at National Oceanography Centre, Southampton, U. K.) [4] Koninklijk Nederlands Meteorologisch Instituut (KNMI), De Bilt, The Netherlands. [5] Fondazione Centro Euro-Mediterraneo sui Cambiamenti Climatici (CMCC), Bologna, Italy. [6] Barcelona Supercomputing Center – Centro Nacional de Supercomputación (BSC), Barcelona, Spain. [7] Centre National de Recherches Météorologiques - Centre Europeen de Recherche et de Formation Avancee en Calcul Scientifique (CNRM-CERFACS), Toulouse, France. [8] CECI, Université de Toulouse, CERFACS/CNRS, Toulouse, France. [9] Max Planck Gesellschaft zur Foerderung der Wissenschaften E.V. (MPI-M), Hamburg, Germany. [10] European Centre for Medium Range Weather Forecasting (ECMWF), Reading, U.K. [11] Penn State University, State College, Pennsylvania, USA. [12] University of California, Davis, Davis, California, USA. [13] JAMSTEC, Tokyo, Japan. [14] Meteorological Research Institute (MRI), Tsukuba, Japan. [15] Texas A&M University, College Station, USA. [16] International Laboratory for High Resolution Earth System

Prediction (iHESP), College Station, USA. [17] National Center for Atmospheric Research (NCAR), Boulder, USA. [18] Qingdao National Laboratory for Marine Science (QNLM), Qingdao, China.

Corresponding author: Malcolm Roberts (malcolm.roberts@metoffice.gov.uk)

Key Points:

- Biases in tropical cyclone distribution, frequency and intensity are generally reduced in models at 25km resolution
- Northern hemisphere basins show mixed responses to future forcing, while Southern Indian Ocean activity projected to decline
- Future changes in 10m wind speed in coupled models are mixed, models with lower bias suggest small increases

Abstract

Future changes in tropical cyclone properties are an important component of climate change impacts and risk for many tropical and mid-latitude countries. In this study we assess the performance of a multi-model ensemble of climate models, at resolutions ranging from 250km to 25km. We use a common experimental design including both atmosphere-only and coupled simulations run over the period 1950-2050, with two tracking algorithms applied uniformly across the models.

There are overall improvements in tropical cyclone frequency, spatial distribution and intensity in models at 25 km resolution, with several of them able to represent very intense storms. Projected tropical cyclone activity by 2050 generally declines in the South Indian Ocean, while changes in other ocean basins are more uncertain and sensitive to both tracking algorithm and imposed forcings. Coupled models with smaller biases suggest a slight increase in average TC 10m wind speeds by 2050.

Plain Language Summary

Tropical cyclones pose great risks to individuals and societies, particularly in terms of their local impacts, and how such risks may change in the future is a key question. In this work we use a common experimental framework with seven different state-of-the-art global climate models, together with two different methods of identifying tropical cyclones. We find that the simulation of tropical cyclone frequency, spatial distribution and intensity in some models approaches observed values with the model grid spacings of 20-50km. Future projections to 2050 suggest activity will generally decline in the South Indian Ocean while a more mixed picture is revealed in other regions.

1 Introduction

The present-day impact of tropical cyclones on life and property are clear (e.g. the MunichRe review, Mahalingham et al., 2018). However their role and interaction with the climate system is still a subject of intense study (for example Dominguez & Magaña, 2018; Franco-Díaz et al., 2019; Guo et al., 2017). Limited theoretical understanding, for instance what limits the present-day annual global frequency to about 100, as well as the fact that our most reliable global observations only cover the last few decades, present a challenge for prediction. Without fundamental understanding, it is difficult to constrain future projections of tropical cyclones.

Some studies have suggested that changes in tropical cyclones are potentially detectable in the present day (Knutson et al., 2019a). Observed changes in intensity (Elsner et al. 2008; Kossin et al. 2013), including the migration of the location of maximum intensity (Altman et al., 2018; Kossin et al. 2014; Sharmila & Walsh, 2018) have been documented, with possible links to frequency (Kang & Elsner, 2015). Evidence for reductions in propagation speeds since 1949 have been suggested (Kossin, 2018) but also questioned (Lanzante, 2019; Moon et al. 2019), while changes in precipitation associated with individual TCs have also been proposed (Emanuel, 2017; Risser & Wehner, 2017; van Oldenborgh et al., 2017). However disentangling natural variability from anthropogenic forcing remains challenging (Knutson et al., 2019a).

Tropical cyclones challenge our current modelling capabilities (see the reviews by Walsh et al., 2015, 2016): they are relatively small scale features, tasking model resolution; their low annual frequency and large variability, from days to decades, require the use of ensembles and long simulations; their sensitivity to the large-scale environment requires minimal model biases.

Several studies (Knutson et al., 2015a; Manganello et al., 2012; Murakami et al., 2015; Roberts et al., 2014; Wehner et al., 2014; Yamada et al., 2017) support the Intergovernmental Panel on Climate Change (IPCC) Fifth Assessment Report (AR5) prediction that the most intense TCs will get more intense while the overall frequency of TCs decreases. The study of Christensen et al. (2013) projects that the frequency of TC activity globally will probably decrease or remain stable. Idealised studies by Emanuel (2013) and Bhatia et al., (2018) differed from most TC model frequency predictions, predicting an increase in the global TC frequency. Even though there is little confidence in the prediction of frequency and intensity for particular regions, the average global TC maximum wind speed and precipitation amount is expected to increase. Studies by Bhatia et al. (2018) and Kim et al. (2014) found that coupled atmosphere-ocean models continue to strongly predict increasing TC intensities in a warmer climate. The record-breaking intensities of recent events such as Typhoon Haiyan of 2013 and the record rainfall of Hurricane Harvey of 2017 are consistent with these inferences.

Even though various studies (Bell et al., 2019; Kim et al., 2014; Knutson et al., 2015; Li et al., 2010; Manganello et al., 2014; Murakami et al., 2015; Nakamura et al., 2017; Park et al., 2017; Roberts et al., 2014; Sugi et al.2017; Wehner et al., 2015; Yamada et al., 2017; Yoshida et al.2017; Zhang & Wang, 2017) have examined how TC tracks might change under future climate warming scenarios, there is no clear agreement on projected changes. For instance, either an eastward or a poleward spread of TC development over the North Pacific basin has been found in several of the aforementioned studies. Other work suggests potential changes to TC precipitation (Emanuel, 2017) and seasonal cycle (Dwyer et al., 2015). Knutson et al., (2019a, 2019b) summarise the latest knowledge of observed changes and modelled future projections.

In this study we present results extracted from new simulations produced as part of the High Resolution Model Intercomparison Project (HighResMIP, Haarsma et al., 2016). We seek to answer the question: How well do these new global models explicitly represent historic tropical cyclone characteristics and does this have implications for projected future changes?

In Section 2 we briefly describe the experiments, models, metrics and tracking algorithms, and section 3 indicates where the data used in this study can be obtained. Our results are described in Section 4 and conclusions are made in Section 5.

2 Methods

2.1 Experimental design

The protocol followed in this study, HighResMIP, is an integral part of the Coupled Model Intercomparison Project (CMIP6, Eyring et al., 2016). HighResMIP differs from standard CMIP6 simulations primarily due to run length (HighResMIP coupled simulations are shorter, atmosphere-only simulations are longer), model complexity (HighResMIP recommends use of standardized aerosol optical properties over time), and some forcings (sea surface temperature and sea-ice are higher frequency and resolution in the atmosphere-only HighResMIP).

Pairs of global model simulations were run, with both atmosphere-only and coupled climate models over the period 1950-2050. The experiments comprise different horizontal resolutions, with minimal parameter changes, using consistent forcing datasets. Such a design allows us to systematically investigate the impact of grid spacing alone on the explicit simulation of tropical

cyclones, both in terms of the past mean state and variability, and future changes, over a time period long enough to sample decadal variability.

The atmosphere-only simulations in HighResMIP are primarily used to test the robustness of the response to the same forcing change across models and resolution. The climate of the coupled models will diverge more strongly, and hence any robust change in these simulations gives insight into common drivers. The future period 2015-2050 uses the high emission SSP585 scenario (O'Neill et al., 2016), which is similar to the CMIP5 RCP8.5 (van Vuuren et al., 2011), in order to enhance the signal, given the small ensemble sizes available (Table S1).

Any experimental design has strengths and weaknesses. The strengths of HighResMIP are: shorter simulations than are required in CMIP6 Diagnostic, Evaluation and Characterization of Klima (DECK) simulations, enabling higher resolution models; the ability to isolate the impact of resolution; the parallel use of atmosphere-only and coupled simulations. There are also weaknesses: the simulations only span 1950-2050, hence the signal to noise may be weak; fewer ensemble members possible for most models, due to the expense of higher resolutions; coupled models only use a short multi-decadal spinup and hence we cannot guarantee the exclusion of model drift; some forcings have been simplified to be more comparable across models, but this does exclude explicit simulation of some drivers of internal variability such as dust.

2.2 Models

The HighResMIP simulations incorporate model resolutions (grid spacing) that range from typical CMIP6 resolutions (~250km in the atmosphere and 100km in the ocean) to considerably higher resolutions (25km atmosphere and 8-25km ocean). The majority of the models used in this study are part of the PRIMAVERA-HighResMIP multi-model ensemble (Roberts et al.,

2020), with both atmosphere-only and coupled model simulations: CNRM-CM6-1 (A Voldoire et al., 2019); ECMWF-IFS (C. D. Roberts et al., 2018); EC-Earth3P (Haarsma et al, 2020); HadGEM3-GC31 (Malcolm J. Roberts et al., 2019); CMCC-CM2-(V)HR4 (Cherchi et al., 2019); MPI-ESM1-2 (Gutjahr et al., 2019). We also include atmosphere-only simulations from NICAM16 (Kodama et al., 2015; Satoh et al., 2014) and MRI-AGCM3-2 (Mizuta et al., 2012), and coupled simulations from CESM1.3 (Small et al., 2014) - tracking results from these models are only available using TempestExtremes (see below). Additional information on the models is provided in the supplementary Table S1.

2.3 Tracking methods

Two complementary tracking algorithms (henceforth trackers) are used to identify model tropical cyclones within the six hourly model output data. They are TRACK (Hodges et al, 2017) and TempestExtremes (Ullrich & Zarzycki, 2017; Zarzycki & Ullrich, 2017). The differences between the trackers are described in Roberts et al., (2020), with each applied in exactly the same way across all the models with no tuning of detection parameters, and no wind speed thresholds are used. This means that we can assess whether any detected changes in tropical cyclones are robust to tracker method as well as model/resolution/experiment combinations, and hence give some indication whether errors are due to model biases or to the trackers themselves. We use trackers that objectively detect simulated TCs rather than from large-scale precursors (e.g. Tory et al., 2013) or basin-scale environments (e.g. Camargo et al., 2020) since we want to evaluate the characteristics of TCs spanning their entire lifetime and their corresponding interaction with the climate system.

2.4 Metrics

165 The TC metrics used in this work are frequency and Accumulated Cyclone Energy (ACE) to
166 diagnose activity, track density to examine spatial distributions, and wind speed for intensity.
167 The frequency (count per year) is the simplest metric of TC activity, but is strongly sensitive to
168 the tracking algorithm, model resolution, observing system changes and other aspects (Roberts et
169 al., 2020). The Accumulated Cyclone Energy (ACE) index (Bell et al., 2000) is an integrated
170 measure of TC activity and its variability is more robust (Scoccimarro et al., 2018; Villarini &
171 Vecchi, 2013; Zarzycki & Ullrich, 2017). We use the same method as Camp et al., (2015) and
172 calculate ACE throughout the lifetime of each model storm during its warm core phase using
173 winds at 925 hPa. Track density is calculated from storm transits per month per 4° cap, and
174 intensity is measured using 10m wind speed at lifetime maximum 925 hPa windspeed.

3 Data

The six hourly model output used for this work is available on the Earth System Grid Federation (ESGF) nodes under references: HadGEM3-GC31 (M. Roberts, 2017b, 2017c, 2017a, 2017d, 2018; Coward & Roberts, 2018; Schiemann et al., 2019), ECMWF-IFS (C D Roberts et al., 2017b, 2017a), CNRM-CM6-1 (Voldoire, 2019b, 2019a), CMCC-CM2-(V)HR4 (Scoccimarro et al., 2017a, 2017b), EC-Earth3P (EC-Earth, 2018, 2019), MPI-ESM1-2 (von Storch et al., 2017b, 2017a), NICAM16 (Kodama et al., 2019a, 2019b), MRI-AGCM3-2 (Mizuta et al., 2019a, 2019b). The CESM1-3 data is not yet available on ESGF.

The storm tracks derived from these datasets and analysed here are available from (M. Roberts, 2019b, 2019a). We have used the time periods 1950-1980 and 2020-2050 to compare future projections against historic performance (tests with 20 or 40 year long periods yield very similar results), and 1979-2014 to compare with observations.

Observed tropical cyclone tracks for the North Atlantic and Eastern Pacific basins are obtained from the National Oceanic and Atmospheric Administration (NOAA) National Hurricane Center's best-track Hurricane Database (HURDAT2 (Jan 2018 version); Landsea & Franklin, 2013). Observed tropical cyclone data for all remaining basins are obtained from the US Navy's Joint Typhoon Warning Centre (JTWC) best-track database (Chu et al., 2002). We define an observed tropical cyclone as having a 1-min maximum sustained wind speed of 34 kt (17.5 m s^{-1}) or higher, to give a globally-uniform criteria, and we exclude subtropical storms from observations.

4 Results

196 The tropical cyclone performance of the models in the historic period will be assessed first, to
197 give some context for the future changes. Roberts et al., (2020) assessed most of the
198 atmosphere-only HighResMIP simulations used here, apart from MRI-AGCM3-2 and
199 NICAM16.

200

201 In the following we will focus on some of the potentially detectable changes in TCs discussed
202 above and test whether there is any robust evidence from our multi-model ensemble.

203 4.1 Tropical cyclone frequency and ACE

204 The tropical cyclone frequency by basin for the 1979-2014 period for the HighResMIP coupled
205 simulations is shown in Fig. 1 using both trackers, with the atmosphere-only simulations shown
206 in Fig. S1 (see also Roberts et al., 2020). Higher resolution models generally have more TCs than
207 their lower resolution counterparts. Some models have very few TCs at any resolution (MPI-
208 ESM1-2), some models have too many (HadGEM3-GC31-HM), and some are close to the
209 observations (ECMWF-HR). The different trackers detect different numbers of storms, with
210 greater disparities at lower resolution. Roberts et al., (2020) showed that, at least for one model
211 at higher resolution, the trackers seemed to converge. This is likely due to storm strength
212 (weaker storms are more likely missed with TempestExtremes), tracker criteria, and the detection
213 variable and criteria (TRACK uses vorticity, TempestExtremes uses mean sea level pressure).

214 Analysis from CMIP5 (Camargo, 2013; Tory et al., 2013) showed that low resolution models
215 have a strong negative bias in the North Atlantic, and this remains true for nearly all the models
216 in this study, particularly when coupled (CNRM-CM6-1 being an exception). Low

intensification rates (Manganello et al., 2012; Roberts et al., 2020) and model physics (Bruyère et al., 2017; Chauvin et al., 2019) may play important roles, probably enhanced in coupled models due to sea surface temperature biases. The improvement at higher resolution may be due to a higher conversion rate of pre-TC seeds into TCs (Vecchi et al., 2019).

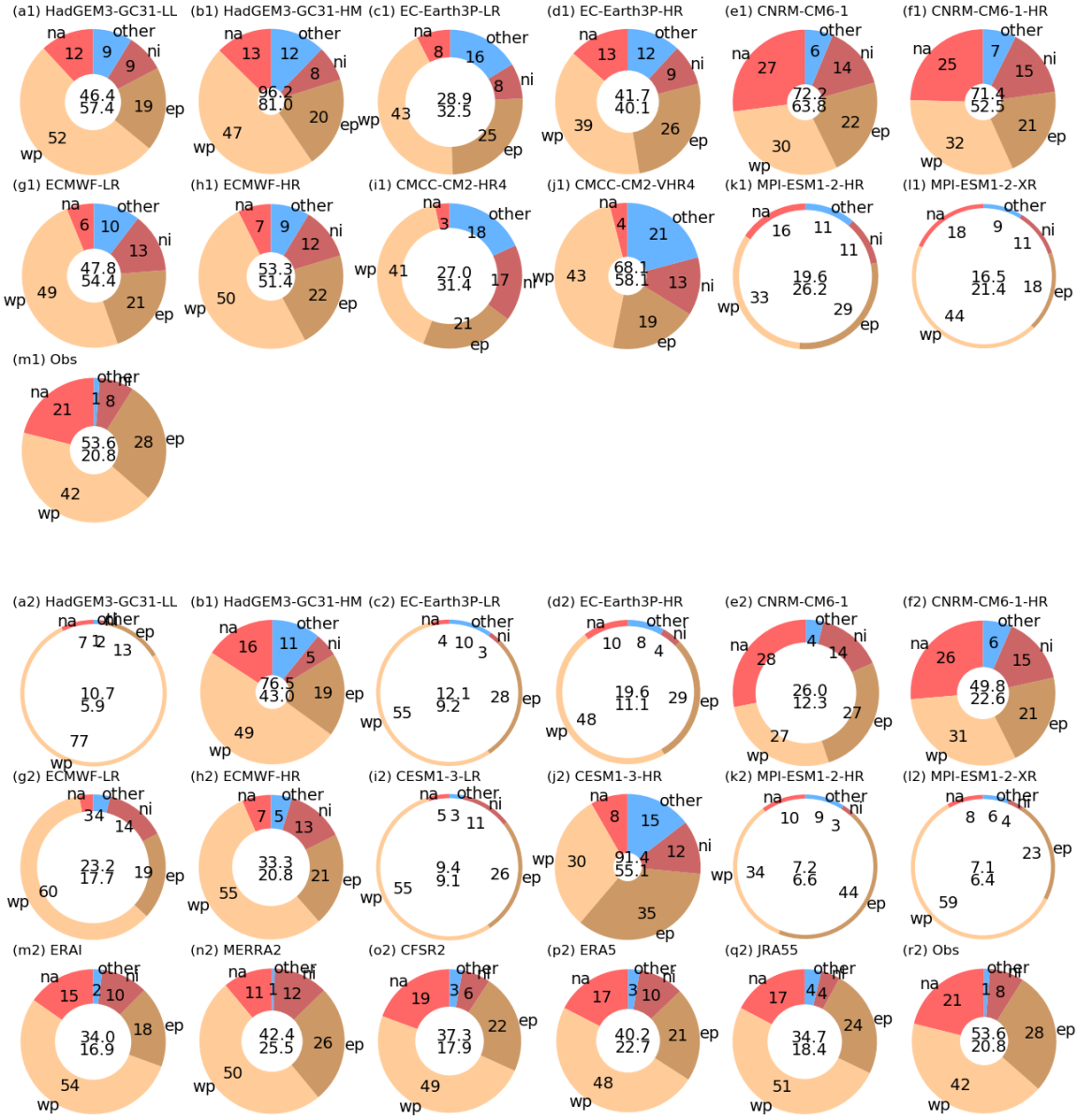

Fig. 1: Tropical cyclone frequency (mean storm counts per year during May-November in Northern Hemisphere, and October-May for the Southern Hemisphere, over 1979-2014 for coupled model simulations and observations, as diagnosed using (a1-q1) the TRACK algorithm and (a2-q2) the TempestExtremes algorithm. The centre of each donut shows the mean number of TCs per year for (NH, SH), with the slices showing percentage of NH storms per basin. The thickness of the donut is scaled to the total NH TC observed frequency (i.e. donuts thicker than duplicate panels (r1,r2) indicate more NH TCs while thinner indicate fewer NH TCs.).

A summary of the multi-model future change in TC activity, as measured by both frequency and ACE, in each ocean basin is shown in Fig. 2 for coupled models and Fig. S2 for atmosphere-only models. Coupled models project a reduction of TC activity in the Southern Hemisphere, with the signal coming largely from changes in the Southern Indian Ocean and Australasian regions as also seen in CMIP5 (Bell et al., 2019; Gleixner et al., 2014; Tory et al., 2013). This result is insensitive to the choice of tracker and is consistent for high and low resolution models and different metrics of cyclone activity (i.e. frequency and ACE). We find no systematic change in cyclone activity across the Northern Hemisphere in coupled simulations. However, the results vary by basin and are more sensitive to the model resolution and choice of tracker compared to the SH. Interestingly, the coupled models show an increase in ACE in the North Atlantic in the lower resolution models whereas in atmosphere-only experiments it is the higher resolution models that show enhanced activity. This emphasizes the uncertainty in projections for this basin, and perhaps an influence of model bias (Fig. 1).

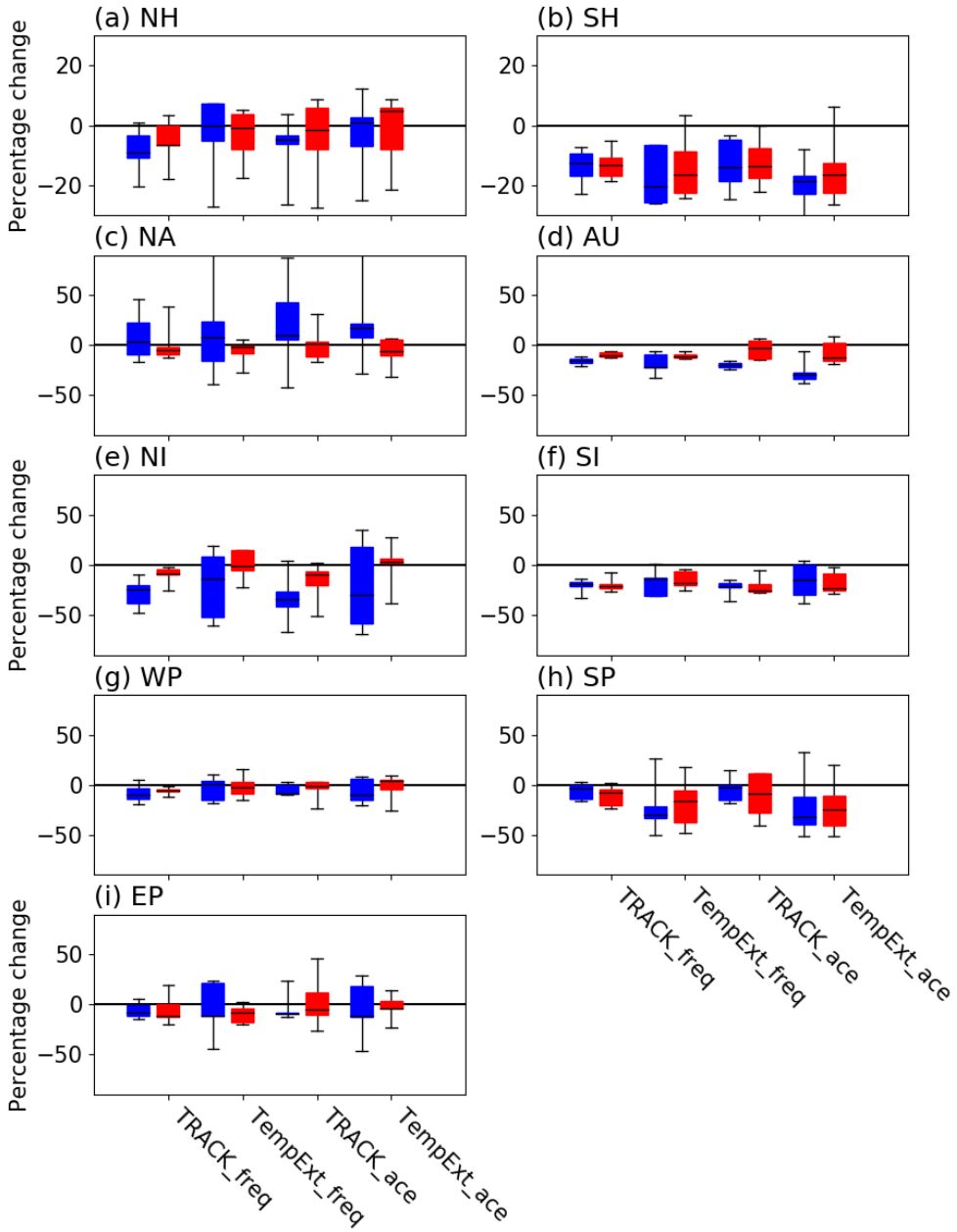

Figure 2: Summary plot for coupled simulations of the percentage differences in activity between future (2020-2050) and historic (1950-1980) periods using four measures, with each bar including data from all models. Blue are lower resolution and red higher resolution groups of models. Metrics are frequency and ACE using TRACK and TempestExtremes (TempExt).

248 ## 4.2 Spatial distribution

249 The multi-model median change in TC track density between historic (1950-1980) and future
250 (2020-2050) time periods is shown in Fig. 3, with the upper panels showing atmosphere-only and
251 the lower coupled model experiments. Results from both trackers are shown, together with an
252 indication of model agreement. For the atmosphere-only simulations (top), the spatial patterns of
253 change are very similar across trackers (Horn et al., 2014), despite the large differences in
254 detection rates shown earlier, and for the most part across resolutions. The only major resolution
255 differences are in the North Atlantic, where there is a larger increase at higher resolution, and a
256 stronger decrease in the North Pacific. There is considerable model agreement in the main areas
257 of change, suggesting that the models' responses to the same projected forcing is robust.

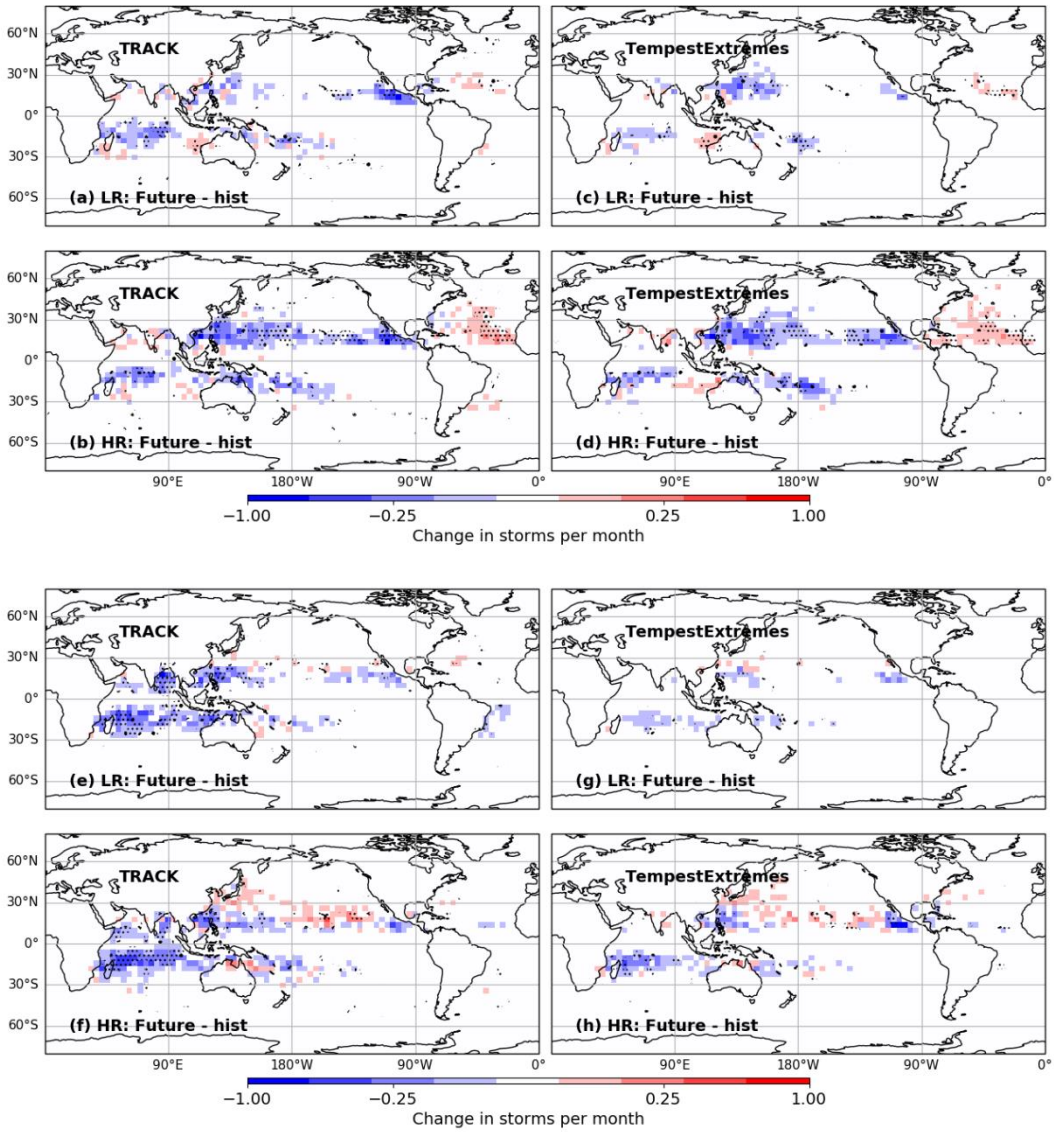

Figure 3: Multi-model mean change in track density between 1950-1980 and 2020-2050, for (top) atmosphere-only and (bottom) coupled model experiments, for (left) TRACK and (right) TempestExtremes trackers. Each plot has the mean of the LR models in the upper panel, and the HR models in the lower panel. Small dots indicate where at least 60% of the models agree on the sign of change, and larger dots show where more than 80% of the models agree on the sign of change.

The spatial changes in the coupled simulations are also consistent across trackers, and indicate a robust decrease in activity in the South Indian Ocean, as also seen in CMIP5 studies (Bell et al., 2019; Gleixner et al., 2014; Knutson et al., 2019b; Tory et al., 2013). In the higher resolution models there is some indication of a poleward shift in activity in the western North Pacific, which would be consistent with Altman et al., (2018), Kossin et al., (2014, 2016) and Sharmila & Walsh, (2018). However, we find a reduction (and/or possibly a polewards shift) in the Eastern Pacific, no signal for change in the North Atlantic and only a very weak signal for poleward shift in the South West Pacific region when using the TRACK tracker.

To contextualise these changes, the spatial biases in the models' TC track densities compared to observations, as well as the individual model changes between historic and future time periods, are shown in Figs. S3, S4 for the TempestExtremes tracker only (similar plots using TRACK have slightly shifted biases but with similar spatial patterns). For the low resolution models, with the exception of NICAM16, there are negative biases in all of the ocean basins for both atmosphere-only and coupled simulations. At higher resolution, the North Atlantic bias generally decreases, and both the East Pacific and the western North Pacific have noticeably increased activity in HadGEM3-GC31, MRI-AGCM3, CNRM-CM6-1 and CESM1-3. In the coupled simulations, HadGEM3-GC31 and CESM1-3 have excessive activity across the central Pacific as well as in parts of the Southern Hemisphere.

4.3 Intensity changes

Many recent studies have indicated that although changes in future tropical cyclone climatology are uncertain, it is likely that intensities (as measured by wind speed and maximum precipitation) of the strongest TCs will increase (Emanuel, 2017; Knutson et al., 2019a, 2019b). However,

modelling such changes is challenging for global climate simulations, in which the horizontal resolution is such that few models can simulate strong (Saffir-Simpson Category 4-5 winds above 58 ms^{-1}) hurricanes, particularly in terms of surface wind speeds (Manganello et al., 2012; Mizuta et al., 2012; Murakami et al., 2015; Wehner et al., 2015). Davis (2018) postulated that properly representing such intense storms requires grid spacings smaller than 25km.

The relationship between the bias in the historic probability density function of TC 10m wind speed (calculated by summing the root mean square (RMS) difference over each 5 ms^{-1} bin between model and observations for the period 1979-2014, as shown in Fig. S5) and the future change at lifetime maximum intensity over all storms between 1950-1980 and 2020-2050 is shown in Fig. 4. The higher resolution models (denoted by triangles) generally have the smaller biases compared to lower resolution. In the atmosphere-only simulations, higher resolution/lower biased models have either no change or reduced future wind speeds, while low resolution/high bias models more typically have increased wind speeds. For the coupled models there is less systematic difference between resolutions, with most models showing no change or small increases.

The pdfs of 10m wind speeds for individual models and observations are shown in Fig. S5 for the historic period 1979-2014. Several of the models (CNRM-CM6-1, CMCC-CM2, CESM1-3, MRI-AGCM3-2, NICAM16) can simulate wind speeds above 50 ms^{-1} and hence Category 3 or higher intensity, with MRI-AGCM3-2-HR extending to 80 ms^{-1}.

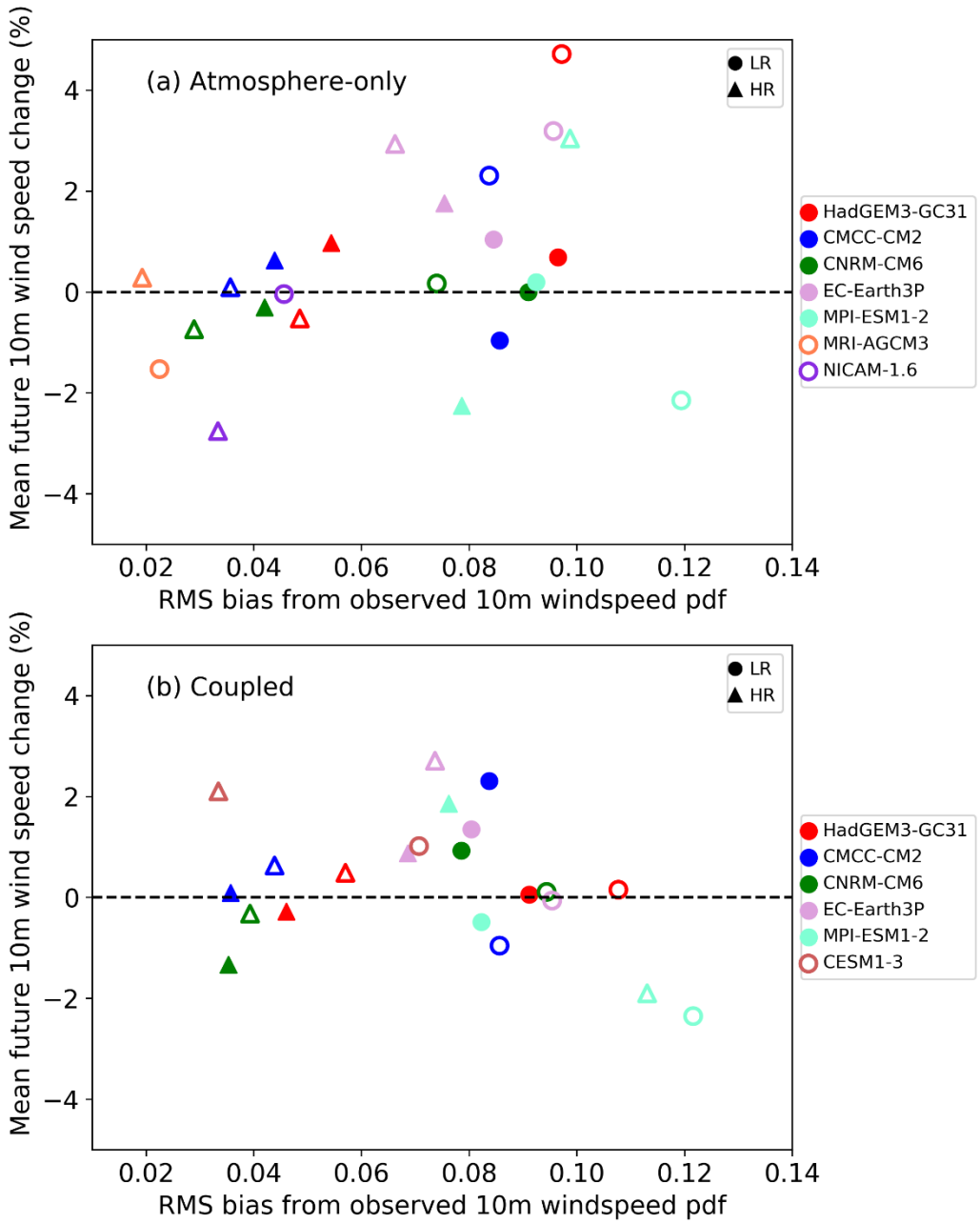

307

308 Figure 4: Scatter plot relating the root mean square bias in 10m wind speed pdf (from Fig. S5)

309 over 1979-2014 to the mean change in 10m wind speed averaged over all TCs at their lifetime

310 maximum intensity between 1950-1980 and 2020-2050 in (a) atmosphere-only and (b) coupled

simulations. The filled symbols use TRACK and the non-filled use TempestExtremes, the circles are the lower resolution (LR) and triangles higher resolution (HR) models.

5 Conclusions

It remains extremely challenging to represent tropical cyclones in global climate simulations over long enough time periods, with enough ensemble members at resolutions sufficient to simulate the most intense storms for the right reasons. Because of the relatively short historical record of observations, presenting their own uncertainties, and due to considerable variability on many timescales, determining any signal due to climate change is difficult.

The models so far analysed following the CMIP6 HighResMIP protocol show a wide variety of behaviours, with some models at 20-50 km resolution able to represent tropical cyclone frequency, spatial distribution and even intensities comparable to observations. Such improved performance adds confidence that such models can provide robust insight into how tropical cyclones might change in future. The North Atlantic remains particularly challenging in the coupled models, even at higher resolution, where the TC frequency is consistently biased low.

We have found several robust changes of tropical cyclones between the historic and future periods. The results suggest a decrease in TC activity in the Southern Hemisphere, more so in the coupled models, particularly in the South Indian Ocean, while changes in the Northern Hemisphere are more mixed. There is some hint of a shift in track positions in some basins consistent with recent observations and modelling. Small increases in 10m wind speeds are found in the coupled models with reduced present-day biases, though less systematic that suggested by other observational and modelling studies. Changes in future projections due to

increased model resolution are relatively modest, though atmosphere-only model wind speeds do have a different sign at low and high resolution.

Given the state-of-the-art models used in this study, it is unclear what factors might cause the results to seem inconsistent with previous work and recent observations. From the modelling perspective these might include: models not retuned for higher resolution; slightly idealised HighResMIP experimental design; inadequate physics or continued lack of resolution and/or ensemble size. However, the relatively short reliable historical record may also be conflating multi-decadal variability and climate change signals. More detailed (process-based) analyses of these simulations, including large-scale circulation changes, may help to better understand these two timescales and lead to more robust projections of future tropical cyclone risk.

Acknowledgments, Samples, and Data

MR and JC acknowledge support from the UK-China Research & Innovation Partnership Fund through the Met Office Climate Science for Service Partnership (CSSP) China as part of the Newton Fund. MR, JS, PLV, KH, BV, RH, AB, ES, LPC, LT, CR, RS, DP acknowledge funding from the PRIMAVERA project, funded by the European Union's Horizon 2020 programme under Grant Agreement no. 641727. JM acknowledges funding from the Blue-Action project, funded by the European Union's Horizon 2020 programme under Grant Agreement no. 727852. Funding for PU and CZ to support use of the TempestExtremes suite was provided under NASA award NNX16AG62G and the US Department of Energy Office of Science award number DE-SC0016605. The CESM1.3 simulations are completed through the International Laboratory for High Resolution Earth System Prediction (iHESP) – a collaboration among QNLM, TAMU and NCAR, from which DF, QZ, GD, NR, HW and LW acknowledge funding. NCAR is a major

facility sponsored by the US National Science Foundation under Cooperative Agreement No. 1852977.

There are no financial conflicts of interest for any author.

The datasets used in this work are cited in this manuscript with appropriate doi's in publically available archives. The tracked datasets are either already available on the CEDA data catalogue (as cited in the manuscript), or currently being archived there.

References

Altman, J., Ukhvatkina, O. N., Omelko, A. M., Macek, M., Plener, T., Pejcha, V., … Dolezal, J. (2018). Poleward migration of the destructive effects of tropical cyclones during the 20th century. *Proceedings of the National Academy of Sciences*, *115*(45), 11543–11548. https://doi.org/10.1073/pnas.1808979115

Bell, G. D., Halpert, M. S., Schnell, R. C., Higgins, R. W., Lawrimore, J., Kousky, V. E., … Artusa, A. (2000). Climate Assessment for 1999. *Bulletin of the American Meteorological Society*, *81*(6), S1–S50. https://doi.org/10.1175/1520-0477(2000)81[s1:CAF]2.0.CO;2

Bell, S. S., Chand, S. S., Tory, K. J., Dowdy, A. J., Turville, C., & Ye, H. (2019). Projections of southern hemisphere tropical cyclone track density using CMIP5 models. *Climate Dynamics*, *52*(9), 6065–6079. https://doi.org/10.1007/s00382-018-4497-4

Bhatia, K., Vecchi, G., Murakami, H., Underwood, S., & Kossin, J. (2018). Projected Response of Tropical Cyclone Intensity and Intensification in a Global Climate Model. *Journal of Climate*, *31*(20), 8281–8303. https://doi.org/10.1175/JCLI-D-17-0898.1

Bruyère, C. L., & Coauthors. (2017). *Impact of Climate Change on Gulf of Mexico Hurricanes*. https://doi.org/10.5065/D6RN36J3

Camargo, S. J. (2013). Global and Regional Aspects of Tropical Cyclone Activity in the CMIP5 Models. *Journal of Climate*, *26*(24), 9880–9902. https://doi.org/10.1175/JCLI-D-12-00549.1

Camargo, S. J., Giulivi, C. F., Sobel, A. H., Wing, A. A., Kim, D., Moon, Y., … Zhao, M. (2020). Characteristics of model tropical cyclone climatology and the large-scale environment. *Journal of Climate*. https://doi.org/10.1175/JCLI-D-19-0500.1

Camp, J., Roberts, M., MacLachlan, C., Wallace, E., Hermanson, L., Brookshaw, A., … Scaife, A. A. A. (2015). Seasonal forecasting of tropical storms using the Met Office GloSea5 seasonal forecast system. *Quarterly Journal of the Royal Meteorological Society*, *141*(691), 2206–2219. https://doi.org/10.1002/qj.2516

Chauvin, F., Pilon, R., Palany, P., & Belmadani, A. (2019). Future changes in Atlantic hurricanes with the rotated-stretched ARPEGE-Climat at very high resolution. *Climate Dynamics*. https://doi.org/10.1007/s00382-019-05040-4

Cherchi, A., Fogli, P. G., Lovato, T., Peano, D., Iovino, D., Gualdi, S., … Navarra, A. (2019). Global Mean Climate and Main Patterns of Variability in the CMCC-CM2 Coupled Model. *Journal of Advances in Modeling Earth Systems*, *11*(1), 185–209. https://doi.org/10.1029/2018MS001369

Coward, A., & Roberts, M. (2018). *NERC HadGEM3-GC31-HH model output prepared for CMIP6 HighResMIP*. https://doi.org/10.22033/ESGF/CMIP6.1822

Davis, C. A. (2018). Resolving Tropical Cyclone Intensity in Models. *Geophysical Research Letters*, *45*(4), 2082–2087. https://doi.org/10.1002/2017GL076966

Dominguez, C., & Magaña, V. (2018). The Role of Tropical Cyclones in Precipitation Over the Tropical and Subtropical North America. *Frontiers in Earth Science*, *6*, 19. https://doi.org/10.3389/feart.2018.00019

Dwyer, J. G., Camargo, S. J., Sobel, A. H., Biasutti, M., Emanuel, K. A., Vecchi, G. A., … Tippett, M. K. (2015). Projected twenty-first-century changes in the length of the tropical cyclone season. *Journal of Climate*, *28*(15), 6181–6192. https://doi.org/10.1175/JCLI-D-14-00686.1

EC-Earth. (2018). *EC-Earth-Consortium EC-Earth3P-HR model output prepared for CMIP6 HighResMIP*. https://doi.org/10.22033/ESGF/CMIP6.2323

EC-Earth. (2019). *EC-Earth-Consortium EC-Earth3P model output prepared for CMIP6 HighResMIP*. https://doi.org/10.22033/ESGF/CMIP6.2322

Elsner, J. B., Kossin, J. P., & Jagger, T. H. (2008). The increasing intensity of the strongest tropical cyclones. *Nature*, *455*(7209), 92–95. https://doi.org/10.1038/nature07234

Emanuel, K. (2017). Assessing the present and future probability of Hurricane Harvey{\textquoteright}s rainfall. *Proceedings of the National Academy of Sciences*, *114*(48), 12681–12684. https://doi.org/10.1073/pnas.1716222114

Emanuel, K. A. (2013). Downscaling CMIP5 climate models shows increased tropical cyclone activity over the 21st century. *Proceedings of the National Academy of Sciences*, *110*(30), 12219–12224. https://doi.org/10.1073/pnas.1301293110

Eyring, V., Bony, S., Meehl, G. A., Senior, C. A., Stevens, B., Stouffer, R. J., & Taylor, K. E. (2016). Overview of the Coupled Model Intercomparison Project Phase 6 (CMIP6) experimental design and organization. *Geoscientific Model Development Discussions*, *9*(5), 1937–1958. https://doi.org/10.5194/gmdd-8-10539-2015

Franco-Díaz, A., Klingaman, N. P., Vidale, P. L., Guo, L., & Demory, M.-E. (2019). The contribution of tropical cyclones to the atmospheric branch of Middle America's hydrological cycle using observed and reanalysis tracks. *Climate Dynamics*, *53*(9), 6145–6158. https://doi.org/10.1007/s00382-019-04920-z

Gleixner, S., Keenlyside, N., Hodges, K., Tseng, W.-L., & Bengtsson, L. (2014). An inter-

hemispheric comparison of the tropical storm response to global warming. *Clim. Dyn.*, *42*, 2147–2157. https://doi.org/10.1007/s00382-013-1914-6

Guo, L., Klingaman, N. P., Vidale, P. L., Turner, A. G., Demory, M.-E., & Cobb, A. (2017). Contribution of Tropical Cyclones to Atmospheric Moisture Transport and Rainfall over East Asia. *Journal of Climate, 30*(10), 3853–3865. https://doi.org/10.1175/JCLI-D-16-0308.1

Gutjahr, O., Putrasahan, D., Lohmann, K., Jungclaus, J. H., von Storch, J.-S., Brüggemann, N., … Stössel, A. (2019). Max Planck Institute Earth System Model (MPI-ESM1.2) for the High-Resolution Model Intercomparison Project (HighResMIP). *Geoscientific Model Development, 12*(7), 3241–3281. https://doi.org/10.5194/gmd-12-3241-2019

Haarsma, R., Acosta, M., Bakhshi, R., & et al. (2020). HighResMIP versions of EC-Earth: EC-Earth3P and EC-Earth3P-HR. Description, model performance, data handling and validation. *Geoscientific Model Development*. https://doi.org/https://doi.org/10.5194/gmd-2019-350

Haarsma, R. J., Roberts, M. J., Vidale, P. L., Senior, C. A., Bellucci, A., Bao, Q., … von Storch, J.-S. (2016). High Resolution Model Intercomparison Project (HighResMIP v1.0) for CMIP6. *Geoscientific Model Development, 9*(11), 4185–4208. https://doi.org/10.5194/gmd-9-4185-2016

Hodges, K., Cobb, A., & Vidale, P. L. (2017). How well are tropical cyclones represented in reanalysis datasets? *Journal of Climate, 30*(14), 5243–5264. https://doi.org/10.1175/JCLI-D-16-0557.1

Horn, M., Walsh, K., Zhao, M., Camargo, S. J., Scoccimarro, E., Murakami, H., … Oouchi, K.

(2014). Tracking Scheme Dependence of Simulated Tropical Cyclone Response to Idealized Climate Simulations. *Journal of Climate*, *27*(24), 9197–9213. https://doi.org/10.1175/JCLI-D-14-00200.1

Kang, N.-Y., & Elsner, J. B. (2015). Trade-off between intensity and frequency of global tropical cyclones. *Nature Climate Change*, *5*(7), 661–664. https://doi.org/10.1038/nclimate2646

Kim, H. S., Vecchi, G. A., Knutson, T. R., Anderson, W. G., Delworth, T. L., Rosati, A., … Zhao, M. (2014). Tropical cyclone simulation and response to CO2 doubling in the GFDL CM2.5 high-resolution coupled climate model. *Journal of Climate*, *27*(21), 8034–8054. https://doi.org/10.1175/JCLI-D-13-00475.1

Knutson, T., Camargo, S. J., Chan, J. C. L., Emanuel, K., Ho, C.-H., Kossin, J., … Wu, L. (2019a). Tropical Cyclones and Climate Change Assessment: Part I: Detection and Attribution. *Bulletin of the American Meteorological Society*, *100*(10), 1987–2007. https://doi.org/10.1175/BAMS-D-18-0189.1

Knutson, T., Camargo, S. J., Chan, J. C. L., Emanuel, K., Ho, C.-H., Kossin, J., … Wu, L. (2019b). Tropical Cyclones and Climate Change Assessment: Part II. Projected Response to Anthropogenic Warming. *Bulletin of the American Meteorological Society*. https://doi.org/10.1175/BAMS-D-18-0194.1

Knutson, T. R., Sirutis, J. J., Zhao, M., Tuleya, R. E., Bender, M., Vecchi, G. A., … Chavas, D. (2015). Global projections of intense tropical cyclone activity for the late twenty-first century from dynamical downscaling of CMIP5/RCP4.5 scenarios. *Journal of Climate*, *28*(18), 7203–7224. https://doi.org/10.1175/JCLI-D-15-0129.1

Kodama, C., Ohno, T., Seiki, T., Yashiro, H., Noda, A. T., Nakano, M., … Sugi, M. (2019a).

MIROC NICAM16-7S model output prepared for CMIP6 HighResMIP highresSST-present. https://doi.org/10.22033/ESGF/CMIP6.5565

Kodama, C., Ohno, T., Seiki, T., Yashiro, H., Noda, A. T., Nakano, M., … Sugi, M. (2019b). *MIROC NICAM16-8S model output prepared for CMIP6 HighResMIP highresSST-present*. https://doi.org/10.22033/ESGF/CMIP6.5566

Kodama, C., Yamada, Y., Noda, A. T., Kikuchi, K., Kajikawa, Y., Nasuno, T., … Sugi, M. (2015). A 20-Year Climatology of a NICAM AMIP-Type Simulation. *Journal of the Meteorological Society of Japan. Ser. II*, *93*(4), 393–424. https://doi.org/10.2151/jmsj.2015-024

Kossin, J. P. (2018). A global slowdown of tropical-cyclone translation speed. *Nature*, *558*(7708), 104–107. https://doi.org/10.1038/s41586-018-0158-3

Kossin, J. P., Emanuel, K. A., & Camargo, S. J. (2016). Past and Projected Changes in Western North Pacific Tropical Cyclone Exposure. *Journal of Climate*, *29*(16), 5725–5739. https://doi.org/10.1175/JCLI-D-16-0076.1

Kossin, J. P., Emanuel, K. A., & Vecchi, G. A. (2014). The poleward migration of the location of tropical cyclone maximum intensity. *Nature*, *509*(7500), 349–352. https://doi.org/10.1038/nature13278

Kossin, J. P., Olander, T. L., & Knapp, K. R. (2013). Trend Analysis with a New Global Record of Tropical Cyclone Intensity. *Journal of Climate*, *26*(24), 9960–9976. https://doi.org/10.1175/JCLI-D-13-00262.1

Landsea, C. W., & Franklin, J. L. (2013). Atlantic Hurricane Database Uncertainty and

Presentation of a New Database Format. *Mon. Weather Rev.*, *141*, 3576–3592. https://doi.org/10.1175/MWR-D-12-00254.1

Lanzante, J. R. (2019). Uncertainties in tropical-cyclone translation speed. *Nature*, *570*(7759), E6–E15. https://doi.org/10.1038/s41586-019-1223-2

Li, T., Kwon, M., Zhao, M., Kug, J.-S., Luo, J.-J., & Yu, W. (2010). Global warming shifts Pacific tropical cyclone location. *Geophysical Research Letters*, *37*(21). https://doi.org/10.1029/2010GL045124

Mahalingham, A., A., C., C., J., J.Z., Y., G., C., & Evan T. (2018). *Impacts of Severe natural Catastrophes on Financial Markets*.

Manganello, J. V, Hodges, K. I., Dirmeyer, B., Kinter, J. L., Cash, B. A., Marx, L., … Wedi, N. (2014). Future Changes in the Western North Pacific Tropical Cyclone Activity Projected by a Multidecadal Simulation with a 16-km Global Atmospheric GCM. *Journal of Climate*, *27*(20), 7622–7646. https://doi.org/10.1175/JCLI-D-13-00678.1

Manganello, J. V, Hodges, K. I., Kinter, J. L., Cash, B. A., Marx, L., Jung, T., … Wedi, N. (2012). Tropical Cyclone Climatology in a 10-km Global Atmospheric GCM: Toward Weather-Resolving Climate Modeling. *Journal of Climate*, *25*(11), 3867–3893. https://doi.org/10.1175/JCLI-D-11-00346.1

Mizuta, R, Yoshimura, H., Murakami, H., Matsueda, M., Endo, H., Ose, T., … Kitoh, A. (2012). Climate simulations using {MRI-AGCM3.2} with 20-km grid. *J. Meteorol. Soc. Jpn*, *90A*, 233–258. https://doi.org/10.2151/jmsj.2012-A12

Mizuta, Ryo, Yoshimura, H., Ose, T., Hosaka, M., & Yukimoto, S. (2019a). *MRI MRI-AGCM3-*

2-H model output prepared for CMIP6 HighResMIP highresSST-future. https://doi.org/10.22033/ESGF/CMIP6.10972

Mizuta, Ryo, Yoshimura, H., Ose, T., Hosaka, M., & Yukimoto, S. (2019b). *MRI MRI-AGCM3-2-S model output prepared for CMIP6 HighResMIP highresSST-future*. https://doi.org/10.22033/ESGF/CMIP6.6740

Moon, I.-J., Kim, S.-H., & Chan, J. C. L. (2019). Climate change and tropical cyclone trend. *Nature*, *570*(7759), E3–E5. https://doi.org/10.1038/s41586-019-1222-3

Murakami, H., Vecchi, G. A., Underwood, S., Delworth, T. L., Wittenberg, A. T., Anderson, W. G., … Zeng, F. (2015). Simulation and Prediction of Category 4 and 5 Hurricanes in the High-Resolution GFDL HiFLOR Coupled Climate Model. *Journal of Climate*, *28*(23), 9058–9079. https://doi.org/10.1175/JCLI-D-15-0216.1

Nakamura, J., Camargo, S. J., Sobel, A. H., Henderson, N., Emanuel, K. A., Kumar, A., … Zhao, M. (2017). Western North Pacific Tropical Cyclone Model Tracks in Present and Future Climates. *Journal of Geophysical Research: Atmospheres*, *122*(18). https://doi.org/10.1002/2017JD027007

O'Neill, B. C., Tebaldi, C., van Vuuren, D. P., Eyring, V., Friedlingstein, P., Hurtt, G., … Sanderson, B. M. (2016). The Scenario Model Intercomparison Project (ScenarioMIP) for CMIP6. *Geoscientific Model Development*, *9*(9), 3461–3482. https://doi.org/10.5194/gmd-9-3461-2016

Park, D.-S. R., Ho, C.-H., Chan, J. C. L., Ha, K.-J., Kim, H.-S., Kim, J., & Kim, J.-H. (2017). Asymmetric response of tropical cyclone activity to global warming over the North Atlantic and western North Pacific from CMIP5 model projections. *Scientific Reports*, *7*(1), 41354.

https://doi.org/10.1038/srep41354

Risser, M. D., & Wehner, M. F. (2017). Attributable Human-Induced Changes in the Likelihood and Magnitude of the Observed Extreme Precipitation during Hurricane Harvey. *Geophysical Research Letters*, *44*(24), 12,412-457,464. https://doi.org/10.1002/2017GL075888

Roberts, Christopher D., Senan, R., Molteni, F., Boussetta, S., Mayer, M., & Keeley, S. P. E. (2018). Climate model configurations of the ECMWF Integrated Forecasting System (ECMWF-IFS cycle 43r1) for HighResMIP. *Geoscientific Model Development*, *11*(9), 3681–3712. https://doi.org/10.5194/gmd-11-3681-2018

Roberts, Christopher David, Senan, R., Molteni, F., Boussetta, S., & Keeley, S. (2017a). *ECMWF ECMWF-IFS-HR model output prepared for CMIP6 HighResMIP*. https://doi.org/10.22033/ESGF/CMIP6.2461

Roberts, Christopher David, Senan, R., Molteni, F., Boussetta, S., & Keeley, S. (2017b). *ECMWF ECMWF-IFS-LR model output prepared for CMIP6 HighResMIP*. https://doi.org/10.22033/ESGF/CMIP6.2463

Roberts, M. (2017a). *MOHC HadGEM3-GC31-HM model output prepared for CMIP6 HighResMIP*. https://doi.org/10.22033/ESGF/CMIP6.446

Roberts, M. (2017b). *MOHC HadGEM3-GC31-LL model output prepared for CMIP6 HighResMIP*. https://doi.org/10.22033/ESGF/CMIP6.1901

Roberts, M. (2017c). *MOHC HadGEM3-GC31-LM model output prepared for CMIP6 HighResMIP*. https://doi.org/10.22033/ESGF/CMIP6.1321

Roberts, M. (2017d). *MOHC HadGEM3-GC31-MM model output prepared for CMIP6 HighResMIP*. https://doi.org/10.22033/ESGF/CMIP6.1902

Roberts, M. (2018). *MOHC HadGEM3-GC31-HH model output prepared for CMIP6 HighResMIP*. https://doi.org/10.22033/ESGF/CMIP6.445

Roberts, M. (2019a). *CMIP6 HighResMIP: Tropical storm tracks as calculated by the TempestExtremes algorithm*. Retrieved from http://catalogue.ceda.ac.uk/uuid/438268b75fed4f27988dc02f8a1d756d

Roberts, M. (2019b). *CMIP6 HighResMIP: Tropical storm tracks as calculated by the TRACK algorithm*. Retrieved from http://catalogue.ceda.ac.uk/uuid/0b42715a7a804290afa9b7e31f5d7753

Roberts, M. J., Camp, J., Seddon, J., Vidale, P. L., Hodges, K., Vanniere, B., … Ullrich, P. (2020). Impact of Model Resolution on Tropical Cyclone Simulation Using the HighResMIP–PRIMAVERA Multimodel Ensemble. *Journal of Climate, 33*(7), 2557–2583. https://doi.org/10.1175/JCLI-D-19-0639.1

Roberts, M J, Vidale, P. L., Mizielinski, M., Demory, M.-E., Schiemann, R., Strachan, J., … Bell, R. (2014). Tropical cyclones in the UPSCALE ensemble of high resolution global climate models. *J. Climate*. https://doi.org/10.1175/JCLI-D-14-00131.1

Roberts, Malcolm J., Baker, A., Blockley, E. W., Calvert, D., Coward, A., Hewitt, H. T., … Vidale, P. L. (2019). Description of the resolution hierarchy of the global coupled HadGEM3-GC3.1 model as used in CMIP6 HighResMIP experiments. *Geoscientific Model Development, 12*(12), 4999–5028. https://doi.org/10.5194/gmd-12-4999-2019

576 Satoh, M., Tomita, H., Yashiro, H., Miura, H., Kodama, C., Seiki, T., … Kubokawa, H. (2014).
577 The Non-hydrostatic Icosahedral Atmospheric Model: description and development.
578 *Progress in Earth and Planetary Science*, *1*(1), 18. https://doi.org/10.1186/s40645-014-
579 0018-1

580 Schiemann, R., Vidale, P. L., Hatcher, R., & Roberts, M. (2019). *NERC HadGEM3-GC31-HM*
581 *model output prepared for CMIP6 HighResMIP*.
582 https://doi.org/10.22033/ESGF/CMIP6.1824

583 Scoccimarro, E., Bellucci, A., & Peano, D. (2017a). *CMCC CMCC-CM2-HR4 model output*
584 *prepared for CMIP6 HighResMIP*. https://doi.org/10.22033/ESGF/CMIP6.1359

585 Scoccimarro, E., Bellucci, A., & Peano, D. (2017b). *CMCC CMCC-CM2-VHR4 model output*
586 *prepared for CMIP6 HighResMIP*. https://doi.org/10.22033/ESGF/CMIP6.1367

587 Scoccimarro, E., Bellucci, A., Storto, A., Gualdi, S., Masina, S., & Navarra, A. (2018). Remote
588 subsurface ocean temperature as a predictor of Atlantic hurricane activity. *Proceedings of*
589 *the National Academy of Sciences*, *115*(45), 11460–11464.
590 https://doi.org/10.1073/pnas.1810755115

591 Sharmila, S., & Walsh, K. J. E. (2018). Recent poleward shift of tropical cyclone formation
592 linked to Hadley cell expansion. *Nature Climate Change*, *8*(8), 730–736.
593 https://doi.org/10.1038/s41558-018-0227-5

594 Small, R. J., Bacmeister, J., Bailey, D., Baker, A., Bishop, S., Bryan, F., … Vertenstein, M.
595 (2014). A new synoptic scale resolving global climate simulation using the Community
596 Earth System Model. *Journal of Advances in Modeling Earth Systems*, *6*(4), 1065–1094.
597 https://doi.org/10.1002/2014MS000363

598 Sugi, M., Murakami, H., & Yoshida, K. (2017). Projection of future changes in the frequency of
599 intense tropical cyclones. *Climate Dynamics*, *49*(1–2), 619–632.
600 https://doi.org/10.1007/s00382-016-3361-7

601 Tory, K. J., Chand, S. S., McBride, J. L., Ye, H., & Dare, R. A. (2013). Projected Changes in
602 Late-Twenty-First-Century Tropical Cyclone Frequency in 13 Coupled Climate Models
603 from Phase 5 of the Coupled Model Intercomparison Project. *Journal of Climate*, *26*(24),
604 9946–9959. https://doi.org/10.1175/JCLI-D-13-00010.1

605 Ullrich, P. A., & Zarzycki, C. M. (2017). TempestExtremes: a framework for scale-insensitive
606 pointwise feature tracking on unstructured grids. *Geoscientific Model Development*, *10*(3),
607 1069–1090. https://doi.org/10.5194/gmd-10-1069-2017

608 van Oldenborgh, G. J., van der Wiel, K., Sebastian, A., Singh, R., Arrighi, J., Otto, F., … Cullen,
609 H. (2017). Attribution of extreme rainfall from Hurricane Harvey, August 2017.
610 *Environmental Research Letters*, *12*(12), 124009. https://doi.org/10.1088/1748-9326/aa9ef2

611 van Vuuren, D. P., Edmonds, J., Kainuma, M., Riahi, K., Thomson, A., Hibbard, K., … Rose, S.
612 K. (2011). The representative concentration pathways: an overview. *Clim. Change*, *109*, 5–
613 37.

614 Vecchi, G. A., Delworth, T. L., Murakami, H., Underwood, S. D., Wittenberg, A. T., Zeng, F.,
615 … Yang, X. (2019). Tropical cyclone sensitivities to CO2 doubling: roles of atmospheric
616 resolution, synoptic variability and background climate changes. *Climate Dynamics*, *53*(9),
617 5999–6033. https://doi.org/10.1007/s00382-019-04913-y

618 Villarini, G., & Vecchi, G. A. (2013). Multiseason lead forecast of the north atlantic power
619 dissipation index (PDI) and accumulated cyclone energy (ACE). *Journal of Climate*,

26(11), 3631–3643. https://doi.org/10.1175/JCLI-D-12-00448.1

Voldoire, A, Saint-Martin, D., Sénési, S., Decharme, B., Alias, A., Chevallier, M., … Waldman, R. (2019). Evaluation of CMIP6 DECK Experiments With CNRM-CM6-1. *Journal of Advances in Modeling Earth Systems*, *11*(7), 2177–2213. https://doi.org/10.1029/2019MS001683

Voldoire, Aurore. (2019a). *CNRM-CERFACS CNRM-CM6-1-HR model output prepared for CMIP6 HighResMIP*. https://doi.org/10.22033/ESGF/CMIP6.1387

Voldoire, Aurore. (2019b). *CNRM-CERFACS CNRM-CM6-1 model output prepared for CMIP6 HighResMIP*. https://doi.org/10.22033/ESGF/CMIP6.1925

von Storch, J.-S., Putrasahan, D., Lohmann, K., Gutjahr, O., Jungclaus, J., Bittner, M., … Roeckner, E. (2017a). *MPI-M MPI-ESM1.2-XR model output prepared for CMIP6 HighResMIP*. https://doi.org/10.22033/ESGF/CMIP6.10290

von Storch, J.-S., Putrasahan, D., Lohmann, K., Gutjahr, O., Jungclaus, J., Bittner, M., … Roeckner, E. (2017b). *MPI-M MPIESM1.2-HR model output prepared for CMIP6 HighResMIP*. https://doi.org/10.22033/ESGF/CMIP6.762

Walsh, K. J. E., Camargo, S. J., Vecchi, G. A., Daloz, A. S., Elsner, J., Emanuel, K., … Henderson, N. (2015). Hurricanes and climate: The U.S. Clivar working group on hurricanes. *Bulletin of the American Meteorological Society*, *96*(6). https://doi.org/10.1175/BAMS-D-13-00242.1

Walsh, K. J. E. E., Mcbride, J. L., Klotzbach, P. J., Balachandran, S., Camargo, S. J., Holland, G., … Sugi, M. (2016). Tropical cyclones and climate change. *Wiley Interdisciplinary*

Reviews: Climate Change, *7*(1), 65–89. https://doi.org/10.1002/wcc.371

Wehner, M. F., Reed, K. A., Li, F., Prabhat, Bacmeister, J., Chen, C.-T., … Jablonowski, C. (2014). The effect of horizontal resolution on simulation quality in the Community Atmospheric Model, CAM5.1. *Journal of Advances in Modeling Earth Systems*, *6*(4), 980–997. https://doi.org/10.1002/2013MS000276

Wehner, M., Prabhat, Reed, K. A., Stone, D., Collins, W. D., & Bacmeister, J. (2015). Resolution Dependence of Future Tropical Cyclone Projections of CAM5.1 in the U.S. CLIVAR Hurricane Working Group Idealized Configurations. *Journal of Climate*, *28*(10), 3905–3925. https://doi.org/10.1175/jcli-d-14-00311.1

Yamada, Y., Satoh, M., Sugi, M., Kodama, C., Noda, A. T., Nakano, M., & Nasuno, T. (2017). Response of Tropical Cyclone Activity and Structure to Global Warming in a High-Resolution Global Nonhydrostatic Model. *Journal of Climate*, *30*(23), 9703–9724. https://doi.org/10.1175/JCLI-D-17-0068.1

Yoshida, K., Sugi, M., Mizuta, R., Murakami, H., & Ishii, M. (2017). Future Changes in Tropical Cyclone Activity in High-Resolution Large-Ensemble Simulations. *Geophysical Research Letters*, *44*(19), 9910–9917. https://doi.org/10.1002/2017GL075058

Zarzycki, C. M., & Ullrich, P. A. (2017). Assessing sensitivities in algorithmic detection of tropical cyclones in climate data. *Geophysical Research Letters*, *44*(2), 1141–1149. https://doi.org/10.1002/2016GL071606

Zhang, C., & Wang, Y. (2017). Projected Future Changes of Tropical Cyclone Activity over the Western North and South Pacific in a 20-km-Mesh Regional Climate Model. *Journal of Climate*, *30*(15), 5923–5941. https://doi.org/10.1175/JCLI-D-16-0597.1

663

664

Figure 1.

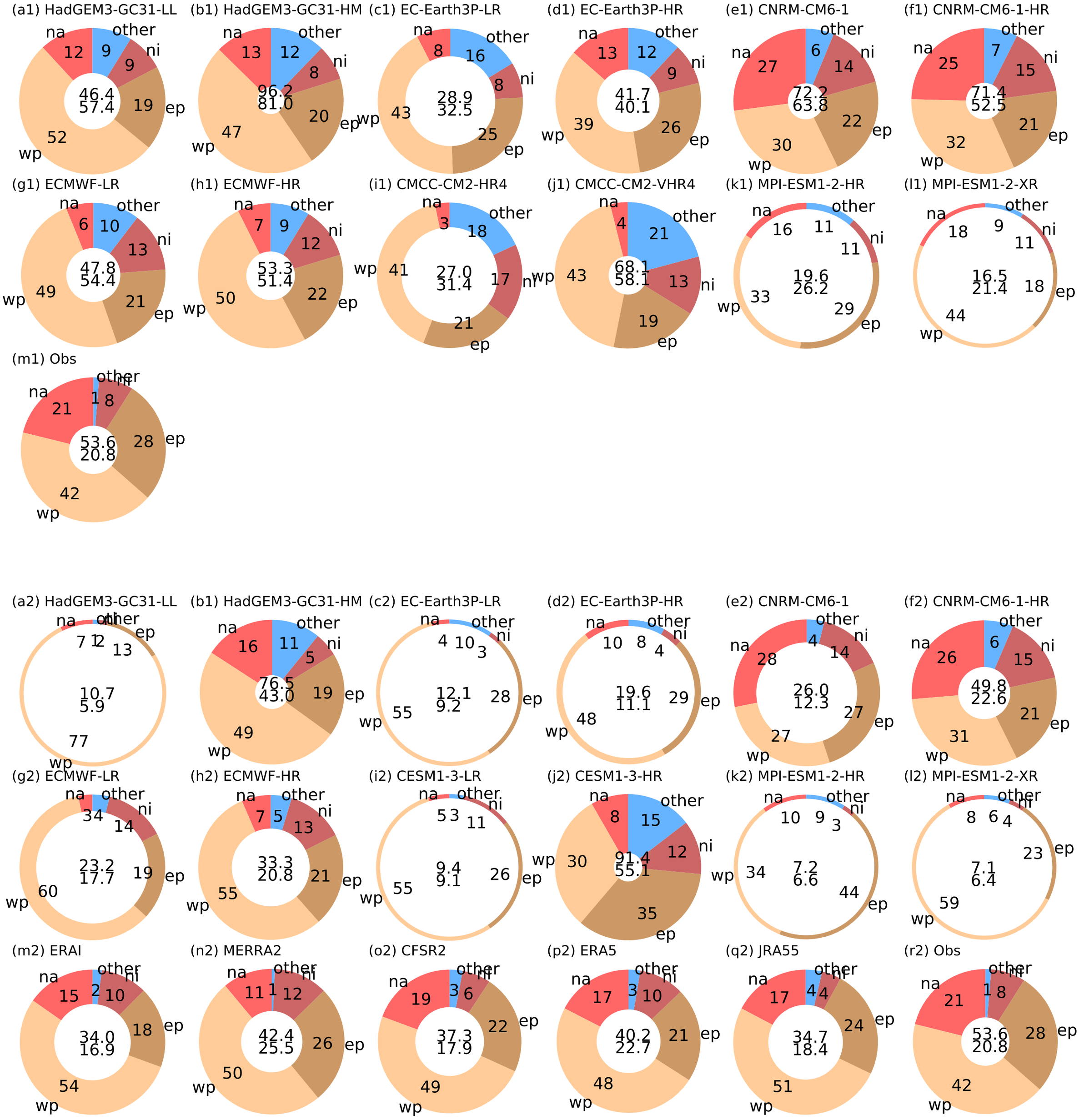
(a1) HadGEM3-GC31-LL
na 12
other 9
ni 9
ep 19
wp 52
46.4
57.4
(b1) HadGEM3-GC31-HM
na 13
other 12
ni 8
ep 20
wp 47
96.2
81.0
(c1) EC-Earth3P-LR
na 8
other 16
ni 8
ep 25
wp 43
28.9
32.5
(d1) EC-Earth3P-HR
na 13
other 12
ni 9
ep 26
wp 39
41.7
40.1
(e1) CNRM-CM6-1
na 27
other 6
ni 14
ep 22
wp 30
72.2
63.8
(f1) CNRM-CM6-1-HR
na 25
other 7
ni 15
ep 21
wp 32
71.4
52.5
(g1) ECMWF-LR
na 6
other 10
ni 13
ep 21
wp 49
47.8
54.4
(h1) ECMWF-HR
na 7
other 9
ni 12
ep 22
wp 50
53.3
51.4
(i1) CMCC-CM2-HR4
na 3
other 18
ni 17
ep 21
wp 41
27.0
31.4
(j1) CMCC-CM2-VHR4
na 4
other 21
ni 13
ep 19
wp 43
68.1
58.1
(k1) MPI-ESM1-2-HR
na 16
other 11
ni 11
ep 29
wp 33
19.6
26.2
(l1) MPI-ESM1-2-XR
na 18
other 9
ni 11
ep 18
wp 44
16.5
21.4
(m1) Obs
na 21
other 1
ni 8
ep 28
wp 42
53.6
20.8
(a2) HadGEM3-GC31-LL
na 7
other 1
ni 2
ep 13
wp 77
10.7
5.9
(b1) HadGEM3-GC31-HM
na 16
other 11
ni 5
ep 19
wp 49
76.5
43.0
(c2) EC-Earth3P-LR
na 4
other 10
ni 3
ep 28
wp 55
12.1
9.2
(d2) EC-Earth3P-HR
na 10
other 8
ni 4
ep 29
wp 48
19.6
11.1
(e2) CNRM-CM6-1
na 28
other 4
ni 14
ep 27
wp 27
26.0
12.3
(f2) CNRM-CM6-1-HR
na 26
other 6
ni 15
ep 21
wp 31
49.8
22.6
(g2) ECMWF-LR
na 34
other 3
ni 14
ep 19
wp 60
23.2
17.7
(h2) ECMWF-HR
na 7
other 5
ni 13
ep 21
wp 55
33.3
20.8
(i2) CESM1-3-LR
na 5
other 3
ni 11
ep 26
wp 55
9.4
9.1
(j2) CESM1-3-HR
na 8
other 15
ni 12
ep 35
wp 30
91.4
55.1
(k2) MPI-ESM1-2-HR
na 10
other 9
ni 3
ep 44
wp 34
7.2
6.6
(l2) MPI-ESM1-2-XR
na 8
other 6
ni 4
ep 23
wp 59
7.1
6.4
(m2) ERAI
na 15
other 2
ni 10
ep 18
wp 54
34.0
16.9
(n2) MERRA2
na 11
other 1
ni 12
ep 26
wp 50
42.4
25.5
(o2) CFSR2
na 19
other 3
ni 6
ep 22
wp 49
37.3
17.9
(p2) ERA5
na 17
other 3
ni 10
ep 21
wp 48
40.2
22.7
(q2) JRA55
na 17
other 4
ni 4
ep 24
wp 51
34.7
18.4
(r2) Obs
na 21
other 1
ni 8
ep 28
wp 42
53.6
20.8

Figure 2.

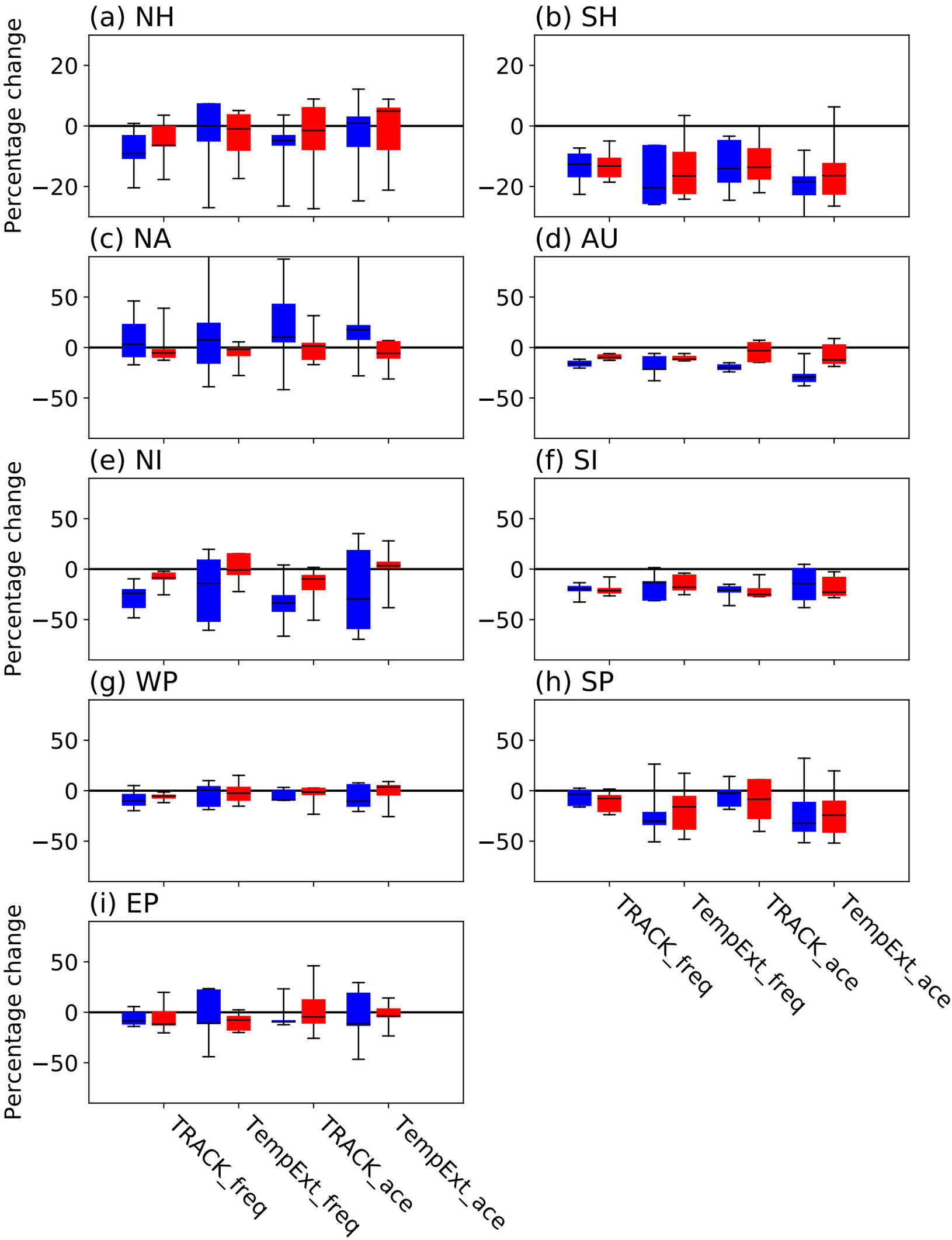
(a) NH
(b) SH
(c) NA
(d) AU
(e) NI
(f) SI
(g) WP
(h) SP
(i) EP
Percentage change
20
0
−20
50
0
−50
TRACK_freq
TempExt_freq
TRACK_ace
TempExt_ace

Figure 3.

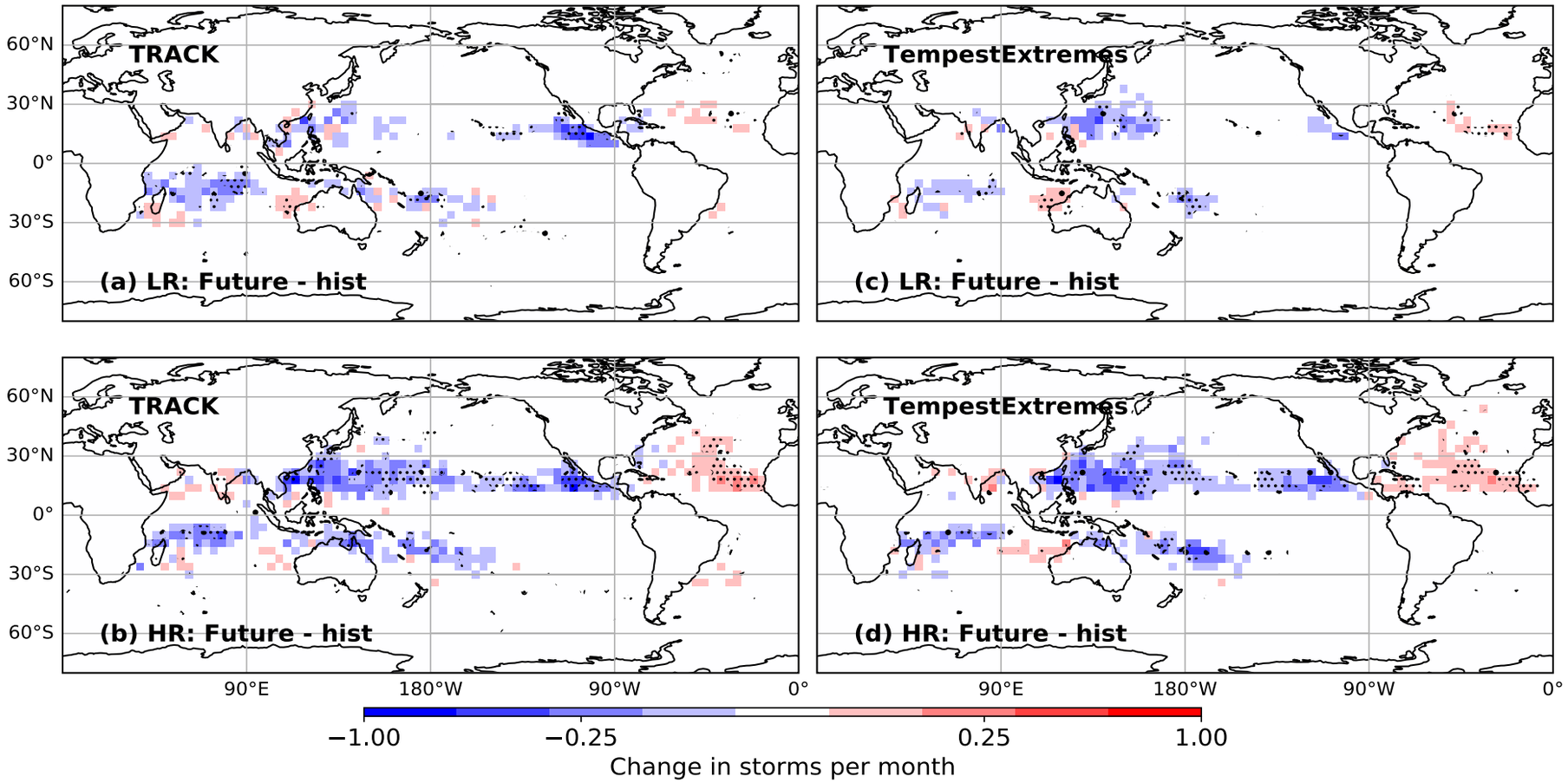
TRACK
TempestExtremes
(a) LR: Future - hist
(c) LR: Future - hist
(b) HR: Future - hist
(d) HR: Future - hist
60°N
30°N
0°
30°S
60°S
90°E
180°W
90°W
0°
−1.00
−0.25
0.25
1.00
Change in storms per month

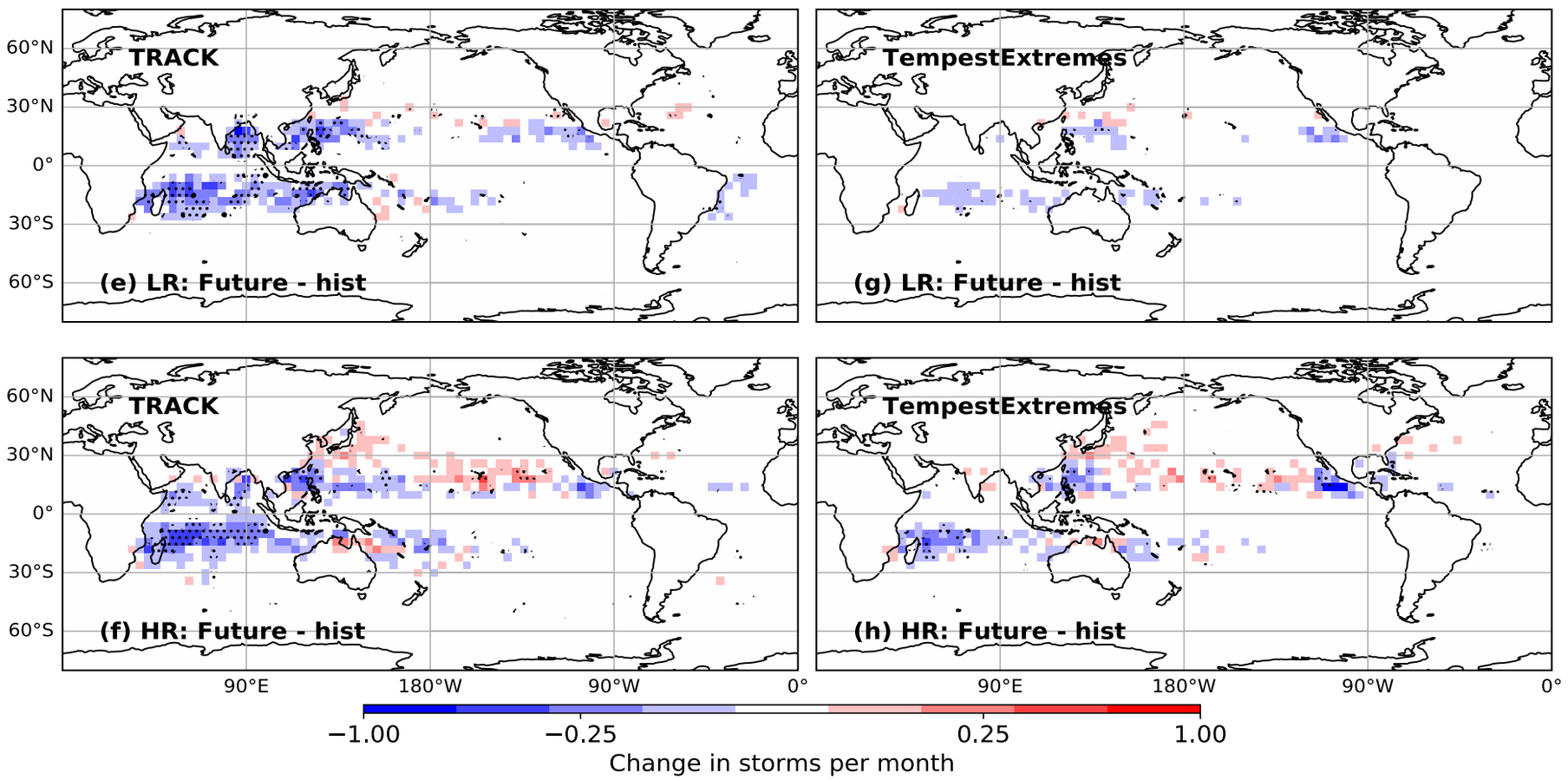
TRACK
TempestExtremes
(e) LR: Future - hist
(g) LR: Future - hist
(f) HR: Future - hist
(h) HR: Future - hist
60°N
30°N
0°
30°S
60°S
90°E
180°W
90°W
0°
−1.00
−0.25
0.25
1.00
Change in storms per month

Figure 4.

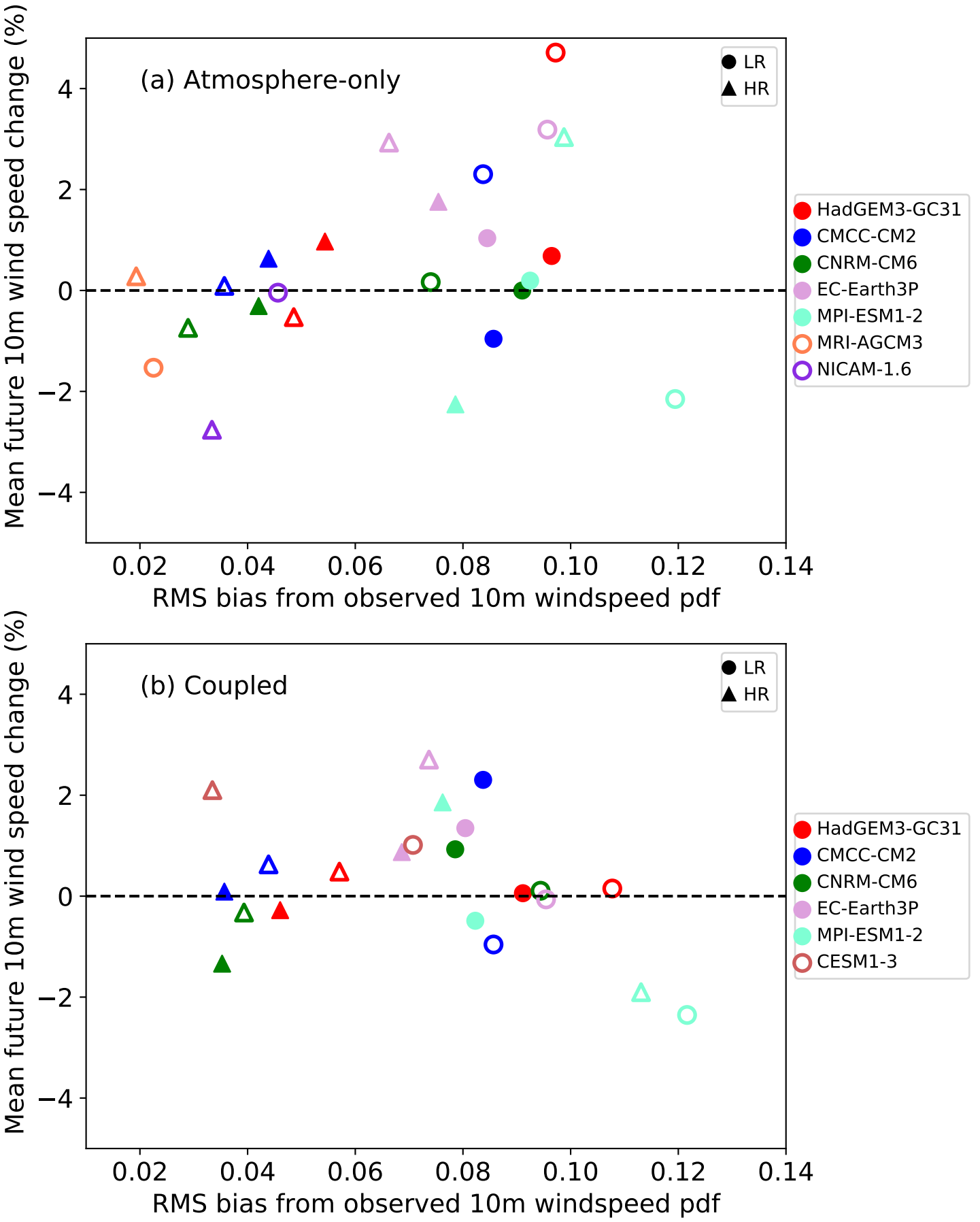
(a) Atmosphere-only
LR
HR
HadGEM3-GC31
CMCC-CM2
CNRM-CM6
EC-Earth3P
MPI-ESM1-2
MRI-AGCM3
NICAM-1.6
Mean future 10m wind speed change (%)
RMS bias from observed 10m windspeed pdf
(b) Coupled
LR
HR
HadGEM3-GC31
CMCC-CM2
CNRM-CM6
EC-Earth3P
MPI-ESM1-2
CESM1-3
Mean future 10m wind speed change (%)
RMS bias from observed 10m windspeed pdf

Geophysical Research Letters

Supporting Information for

Projected Future Changes in Tropical Cyclones using the CMIP6 HighResMIP Multi-model Ensemble

Malcolm John Roberts[1], Joanne Camp[1], Jon Seddon[1], Pier Luigi Vidale[2], Kevin Hodges[2], Benoit Vanniere[2], Jenny Mecking[3], Rein Haarsma[4], Alessio Bellucci[5], Enrico Scoccimarro[5], Louis-Philippe Caron[6], Fabrice Chauvin[7], Laurent Terray[8], Sophie Valcke[8], Marie-Pierre Moine[8], Dian Putrasahan[9], Christopher Roberts[10], Retish Senan[10], Colin Zarzycki[11], Paul Ullrich[12] , Yohei Yamada[13], Ryo Mizuta[14], Chihiro Kodama[13], Dan Fu1[5,16] Qiuying Zhang[15,16], Gokhan Danabasoglu[17,16], Nan Rosenbloom[17,16], Hong Wang[18,16], Lixin Wu[18,16]

1 Met Office, Exeter EX1 3PB, U.K. 2 National Centre for Atmospheric Science (NCAS), University of Reading, Reading, U.K. 3 University of Southampton, Southampton, U.K. (now at National Oceanography Centre, Southampton, U. K.) 4 Koninklijk Nederlands Meteorologisch Instituut (KNMI), De Bilt, The Netherlands. 5 Fondazione Centro Euro-Mediterraneo sui Cambiamenti Climatici (CMCC), Bologna, Italy. 6 Barcelona Supercomputing Center – Centro Nacional de Supercomputación (BSC), Barcelona, Spain. 7 Centre National de Recherches Météorologiques - Centre Europeen de Recherche et de Formation Avancee en Calcul Scientifique (CNRM-CERFACS), Toulouse, France. 8 CECI, Université de Toulouse, CERFACS/CNRS, Toulouse, France. 9 Max Planck Gesellschaft zur Foerderung der Wissenschaften E.V. (MPI-M), Hamburg, Germany. 10 European Centre for Medium Range Weather Forecasting (ECMWF), Reading, U.K. 11 Penn State University, State College, Pennsylvania, USA. 12 University of California, Davis, Davis, California, USA. 13 JAMSTEC, Tokyo, Japan. 14 Meteorological Research Institute (MRI), Tsukuba, Japan. 15 Texas A&M University, College Station, USA. 16 International Laboratory for High Resolution Earth System Prediction (iHESP), College Station, USA. 17 National Center for Atmospheric Research (NCAR), Boulder, USA. 18 Qingdao National Laboratory for Marine Science (QNLM), Qingdao, China.

Contents of this file

Introduction

This material is additional detail that complements the main manuscript. We describe the forcings used by the model simulations and properties of those models. There are extra figures to show changes in individual models to help understand the multi-model means and medians.

Text S1

Forcing datasets

The CMIP6 HighResMIP (Haarsma et al. 2016) historic atmosphere-only forcings (experiment *highresSST-present*) were described in Roberts et al. (2020). Here we describe the coupled model forcings, together with the future forcing.

For nearly all models, the HighResMIP recommendations have been followed for the forcing datasets (Haarsma et al. 2016), including using simplified aerosol optical properties. These optical properties are a combination of a model constant background natural aerosol (typically diagnosed from a pre-industrially-forced simulation), together with time-varying volcanic and anthropogenic aerosol from the Max Planck Institute Aerosol Climatology version 2 (MACv2-SP; Stevens et al. 2015) scheme. The latter uses sulphate aerosol patterns to scale the aerosol forcing magnitude over time. Note that this forcing by design excludes other natural aerosol variability (such as dust) and hence the simulations do not explicitly account for any variability driven by such forcing (Reed et al. 2019), apart from that which is integrated in the SST forcing itself. The exception to this is the CNRM-CM6-1 model, which uses its own aerosol scheme (Voldoire et al. 2019).

The CMIP6 (Eyring et al. 2016) historic, time-varying forcings for solar (Matthes et al. 2017), ozone concentration (Hegglin et al. 2016) and greenhouse gases (GHG) (Meinshausen and Vogel 2016) are used. The land surface properties and land use remain constant, representative of the year 2000 using a repeating seasonal cycle. Future forcings use the CMIP6 SSP585 scenario from 2015-2050.

HighResMIP produced a future SST and sea-ice dataset for 2015-2050 by combining large-scale patterns of warming from a group of CMIP5 RCP8.5 coupled simulations, together with a base state and interannual variability from the historic observed data. This is not meant to represent a real future projection, but is a way to test whether models respond in a similar way to a given future forcing, in contrast to coupled models where the atmosphere-ocean-sea-ice system is free to evolve to a different mean state.

Text S2

Additional information on atmosphere-only simulations

The NICAM16 model is notable for its large TC frequencies (see Fig. S1), and this is likely due to having no convective parameterisation and hence a stronger likelihood of a warm

core signal in geopotential height between 500-250 hPa due to column uplift. As noted previously, the trackers have been applied uniformly across the models rather than being tuned individually.
The changes in activity in the atmosphere-only future projections are shown in Fig. S2.

Text S3

Individual model performance

The track density bias and future change for each individual model is shown in Fig. S3 and S4 for atmosphere-only and coupled model simulations respectively. It is the median values at each point from the figures in columns 2 and 4 that make Fig. 3.
The normalized probability density function (pdf) of 10m wind speeds at peak intensity from each model for the period 1979-2014 are shown in Fig. S5, together with observations. The bias value used in Fig. 4 is derived by summing the root mean square error between model and observations over each 5 ms^{-1} bin.
The pdfs of the difference in 10m wind speeds between periods 2020-2050 and 1950-1980 are shown in Fig. S6. There is no clear signal of an increase in more intense storms at the expense of weaker ones across the multi-model ensemble.

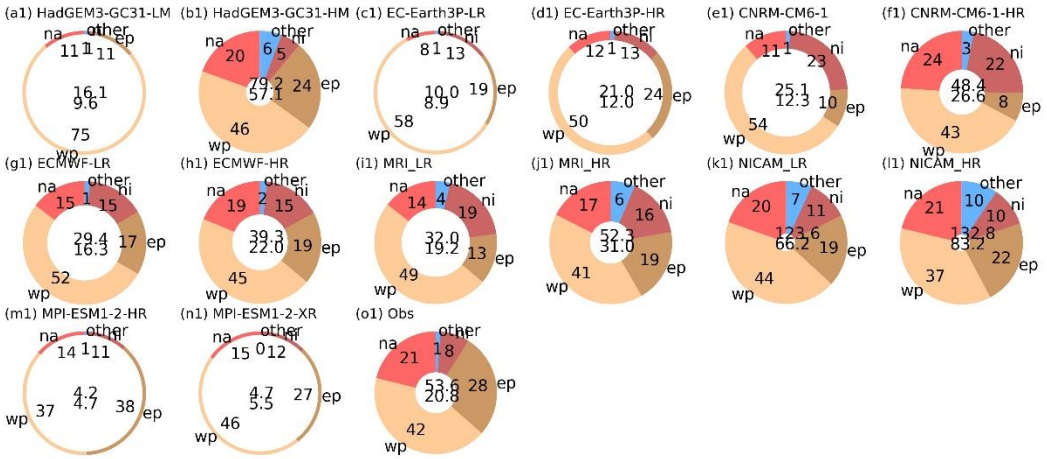

Figure S1. Tropical cyclone frequency (mean storms per year during May-November in Northern Hemisphere, and October-May for the Southern Hemisphere, for HighResMIP atmosphere-only simulations meaned over 1979-2014 from models, as diagnosed using the TempestExtremes algorithm, and observations. The donut chart is divided into ocean basins, the totals in the centre are (NH, SH) mean storm counts per year. The thickness of the donut is scaled to the total NH TC observed frequency (i.e. donuts thicker than in panel (o1) indicate more NH TCs while thinner indicate fewer NH TCs.). Most of these models are shown in Roberts et al. 2020 but now including MRI-AGCM3-2 and NICAM16.

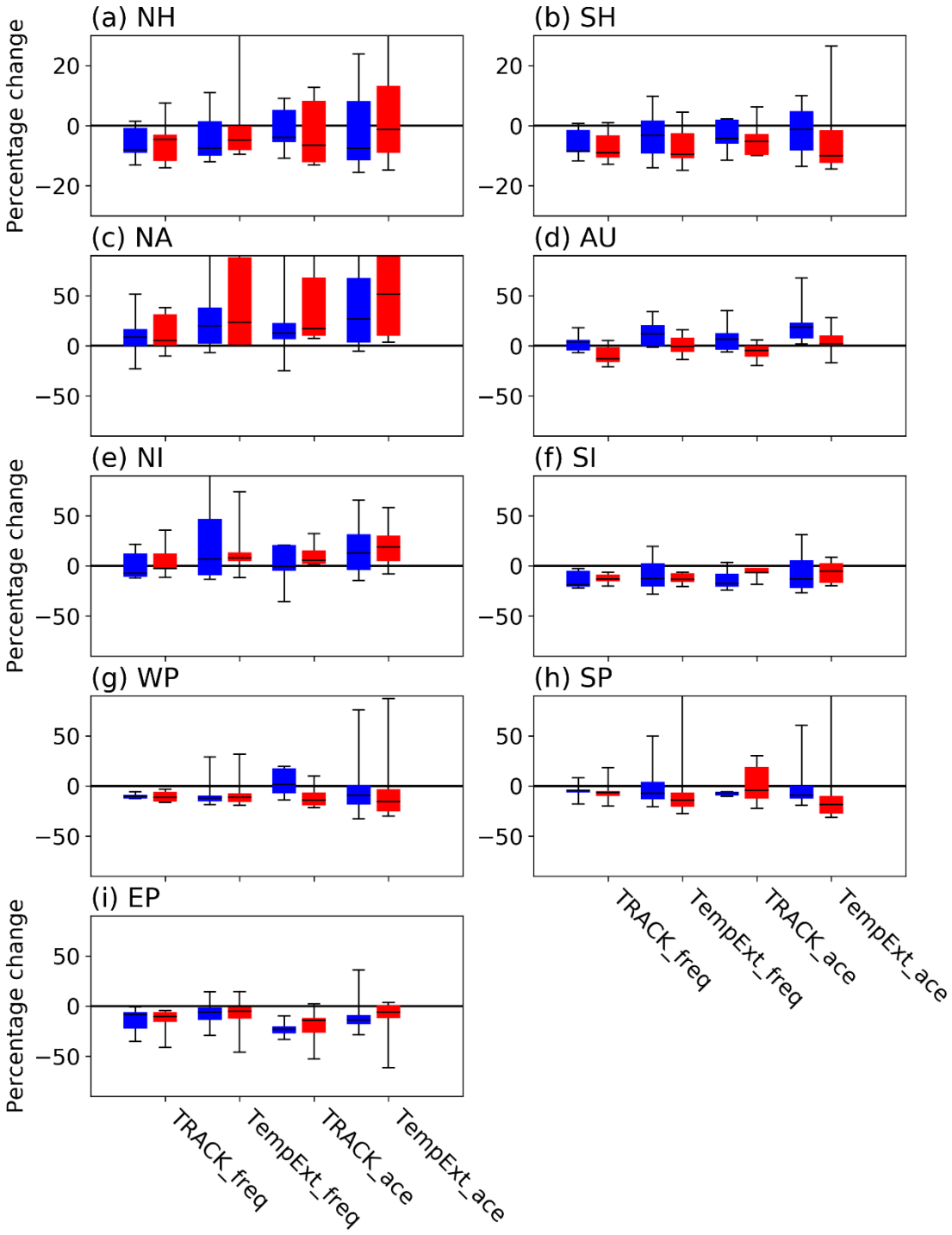

Figure S2: Summary plot for atmosphere-only simulations of the percentage differences in activity between future (2020-2050) and historic (1950-1980) periods using four measures, with each bar including data from all models. Blue are lower resolution and red higher resolution groups of models. Metrics are: (frequency and ACE) using TRACK and TempestExtremes (TempExt).

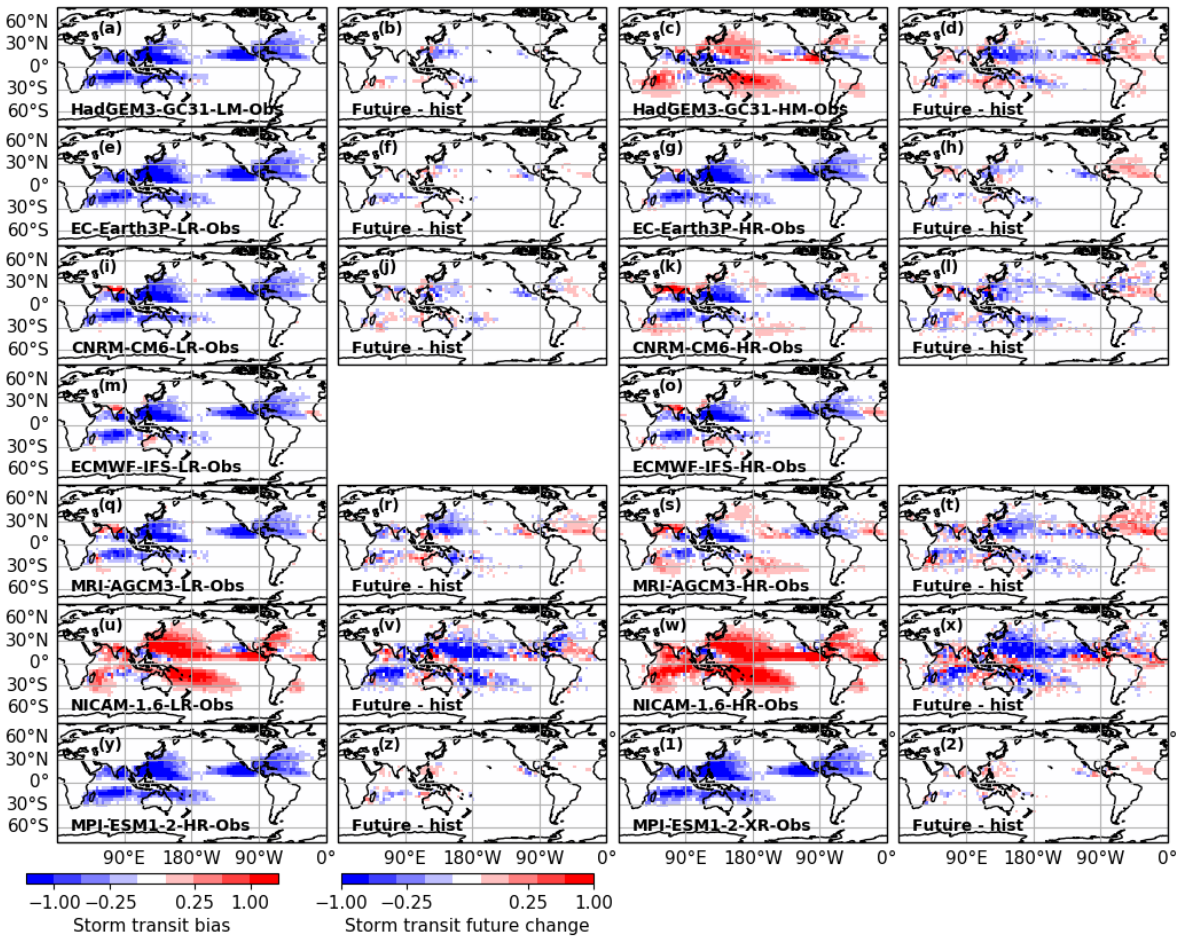

Figure S3. Model tropical cyclone track density (storm transits per month per 4 degree cap) from atmosphere-only simulations using TempestExtremes: for each pair of models, the bias for model in the historic period (1979-2014), and the difference between future – historic (2020-2050 – 1950-1980), are shown respectively. The observed period used is 1979-2014. Note ECMWF does not have future simulation data, and CMCC-CM2-(V)HR4 does not contain the required diagnostics for TempestExtremes.

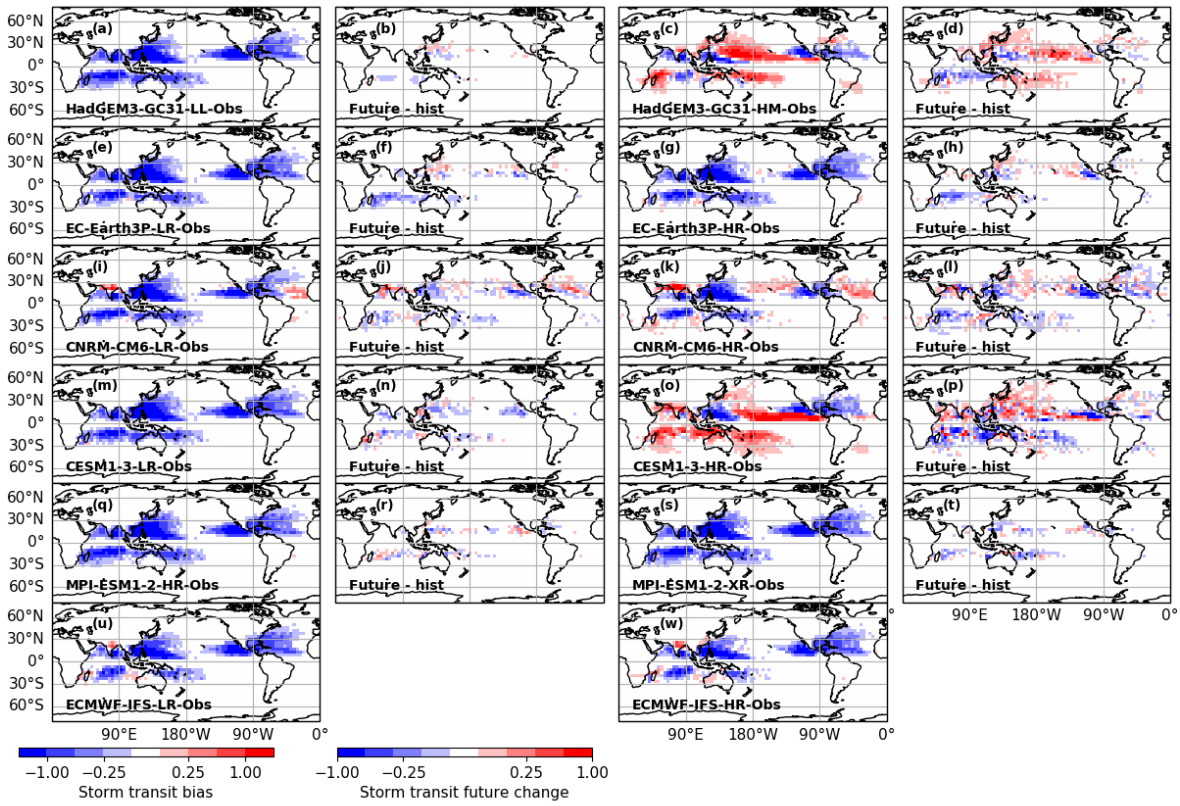

Figure S4. As Fig. S3 but for coupled simulations using TempestExtremes.

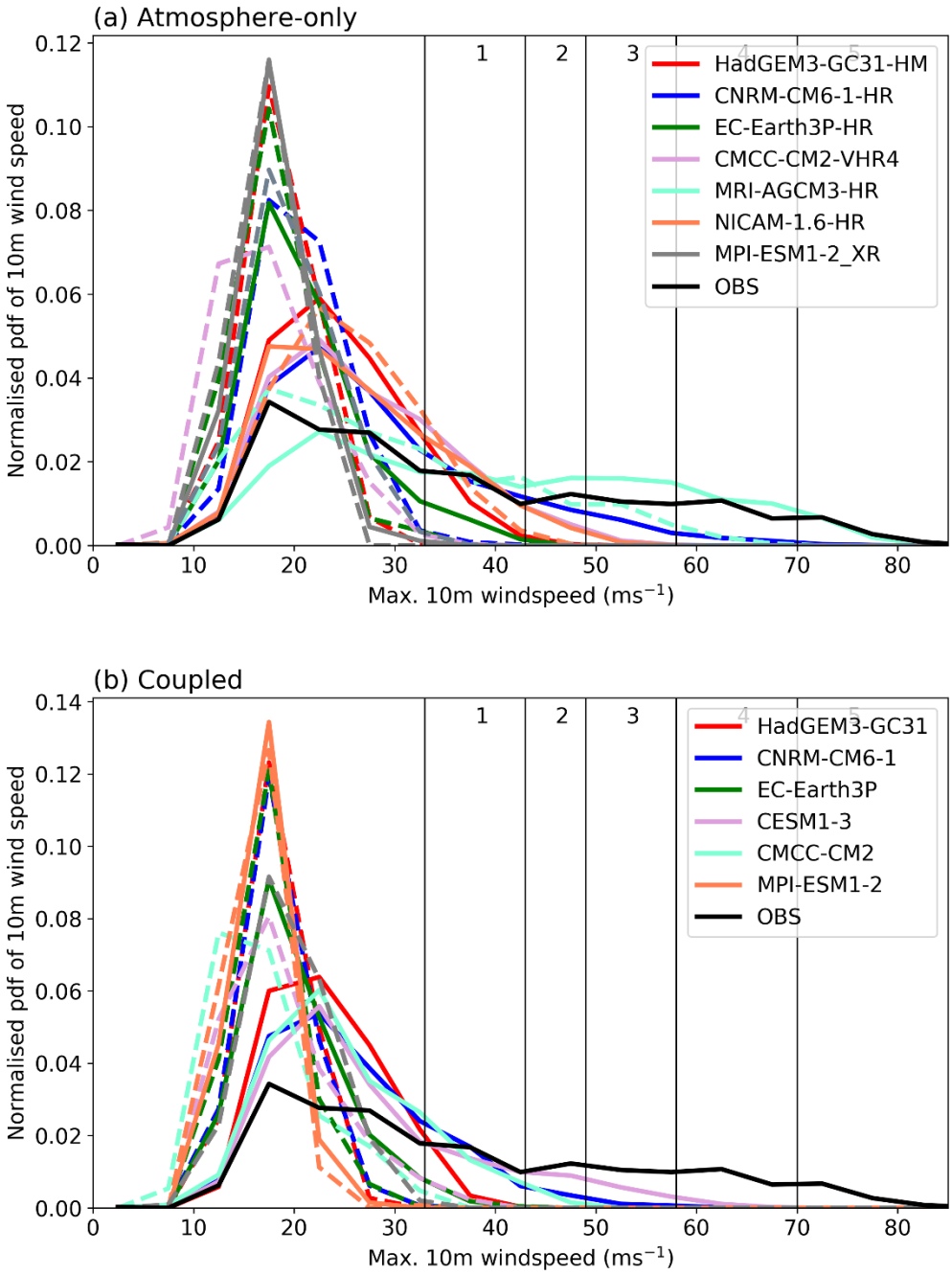

Figure S5. Pdf of 10m wind speed from (a) atmosphere-only and (b) coupled simulations over the period 1979-2014 using TempestExtremes (apart from CMCC-CM2 which uses TRACK).

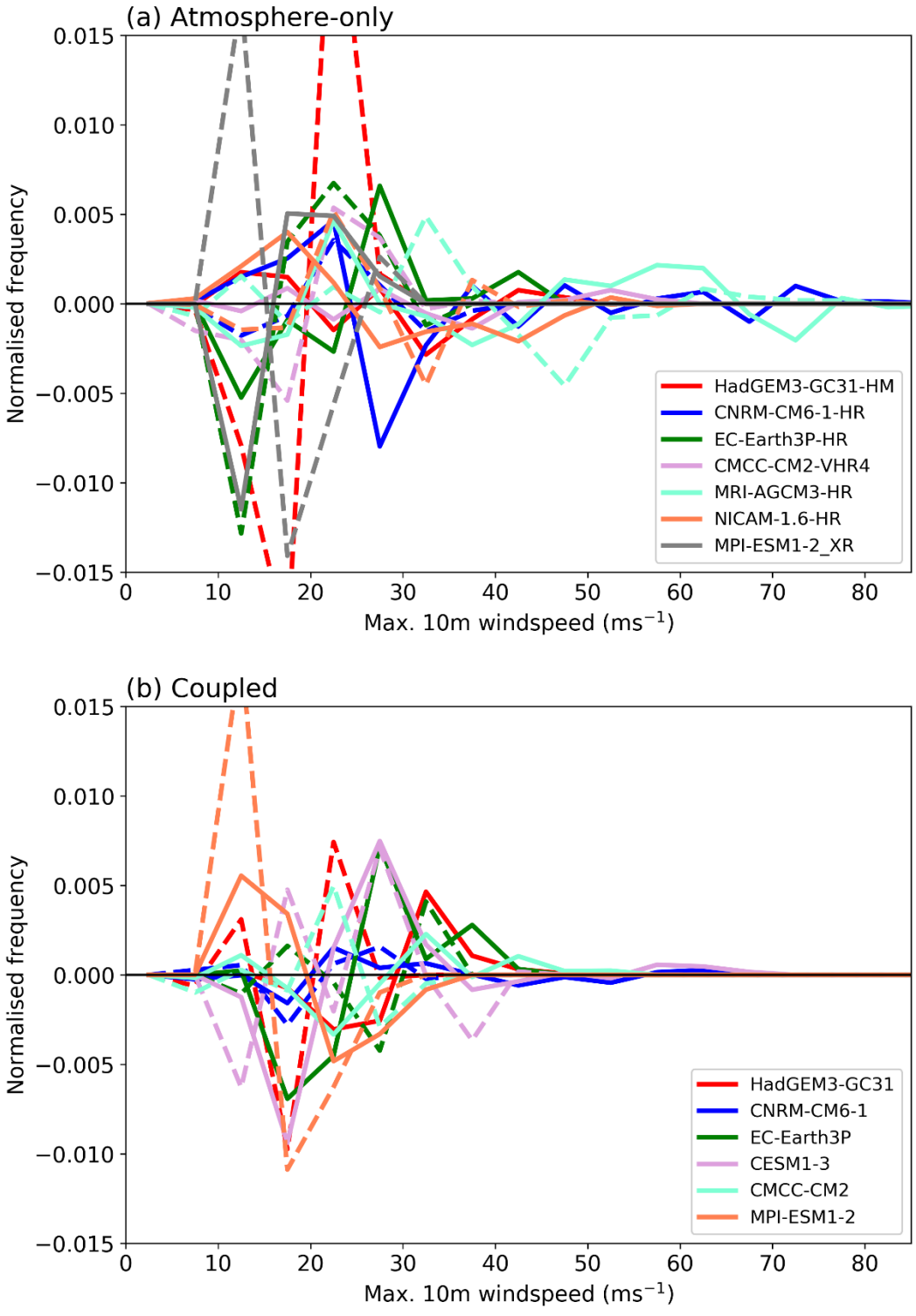

Figure S6. Change in the 10m wind speed pdf between 1950-1985 and 2015-2050 in (a) atmosphere-only and (b) coupled simulations. The dashed lines show the lower resolution models, and the solid lines the higher resolution models.

Institution	MOHC, UREAD, NERC	EC-Earth KNMI, SHMI, BSC, CNR	CERFACS	MPI-M	CMCC	ECMWF	NICAM	MRI	CESM
Model name	HadGEM3-GC31	EC-Earth3P	CNRM-CM6-1	MPI-ESM1-2	CMCC-CM2-(V)HR4	ECMWF-IFS	NICAM16	MRI-AGCM3-2	CESM1-3
Resolution names	LM, MM, HM	LR, HR	LR, HR	HR, XR	HR4, VHR4	LR, HR	7S, 8S	H, S	LL, HH
Model atmosphere	MetUM	IFS cyc36r4	ARPEGE 6.3	ECHAM6.3	CAM4	IFS cyc43r1	NICAM16	MRI-AGCM3-2	CAM5
Atmos dynamical scheme (grid)	Grid point (SISL, lat-lon)	Spectral (linear, reduced Gaussian)	Spectral (linear, reduced Gaussian)	Spectral (triangular, Gaussian)	Grid point (finite volume, lat-lon)	Spectral (cubic octohedral, reduced Gaussian)	non-hydrostatic, icosahedral, finite volume	Spectral (linear, Gaussian)	Finite volume, spectral element
Atmos grid name	N96, N216, N512	Tl255, Tl511	Tl127, Tl359	T127, T255	1°x1°, 0.25°x0.25°	Tco199, Tco399	glevel-7, 8	Tl319, Tl959	1.25°x0.9°, 0.25°x0.25°
Atmos mesh spacing (0N), km	208, 93, 39	78, 39	156, 55	100, 52	100, 28	50, 25	56, 28	60, 20	100, 28
Atmos nominal res (CMIP6)	250, 100, 50	100, 50	250, 50	100, 50	100, 25	50, 25	100, 50	50, 25	100, 25
Atmos model levels (top)	85 (85 km)	91 (0.01 hPa)	91 (78.4 km)	95 (0.01 hPa)	26 (2 hPa)	91 (0.01 hPa)	40 km	64 (0.01 hPa)	30 (3 hPa)
Ocean resol (degree)	1, 0.25, 0.08	1, 0.25	1, 0.25	0.4, 0.4	0.25, 0.25	1, 0.25	N/A	N/A	1, 0.1
Analysis grid	Native	Regrid 0.7x0.7, 0.35x0.35	Regrid 1.4x1.4, 0.5x0.5	Native	Native	Regrid 1x1, 0.5x0.5	Regrid	Native	Native

Ensemble size	3	3	1	1	1	3	1	1	1

Table S1. Summary of models and their properties as used in this work following the CMIP6 HighResMIP experiment design. SISL = semi-implicit, semi-Lagrangian.

References

Meinshausen, M., and Vogel, E.: input4MIPs.UoM.GHGConcentrations.CMIP.UoM-CMIP-1-2-0, Version 20160830, Earth System Grid Federation, https://doi.org/10.22033/ESGF/input4MIPs.1118, 2016.

Hegglin, M., Kinnison, D., Lamarque, J.-F., and Plummer, D.: CCMI ozone in support of CMIP6 – version1.0, Version 20160711, Earth System Grid Federation, https://doi.org/10.22033/ESGF/input4MIPs.1115, 2016.
Matthes, K., Funke, B., Kruschke, T., and Wahl, S.: input4MIPs.SOLARIS-HEPPA.solar.CMIP.SOLARIS-HEPPA-3-2. Version20170103. Earth System Grid Federation, https://doi.org/10.22033/ESGF/input4MIPs.1122, 2017.

Stevens, B., Fiedler, S., Kinne, S., Peters, K., Rast, S., Müsse, J.,Smith, S. J., and Mauritsen, T.: MACv2-SP: a parameterization of anthropogenic aerosol optical properties and an associated Twomey effect for use in CMIP6, Geosci. Model Dev., 10, 433–452, https://doi.org/10.5194/gmd-10-433-2017, 2017.